BONDED CONCRETE OVERLAY OF ASPHALT PAVEMENTS MECHANISTIC-EMPIRICAL DESIGN GUIDE (BCOA-ME)

THEORY MANUAL

University of Pittsburgh
Department of Civil and Environmental Engineering
Pittsburgh, Pennsylvania 15261

Authors:
Zichang Li
Nicole Dufalla
Feng Mu
Julie M. Vandenbossche, Ph.D., P.E.

Funded by:
FHWA Pooled Fund Study TPF 5-165

Additions (Faulting model, July 2021):
Sushobhan Sen, Ph.D.
John DeSantis, Ph.D.
Charles Donnelly

Funded by:
Pennsylvania Department of Transportation
California Department of Transportation
National Road Research Alliance

Sept. 2013

(Last Revised: December 2021)

Acknowledgements

The authors would like to thank the Iowa, Kansas, Minnesota, Missouri, Mississippi, New York, South Dakota, North Carolina, Pennsylvania, and Texas Departments of Transportation. These states are all participating in the FHWA Pooled Fund Study TPF 5-165 under which the BCOA-ME was developed.

The authors would like to thank the California Department of Transportation for funding that initiated the development of the faulting model. The authors greatly appreciate the support of Lydia Peddicord and the Pennsylvania Department of Transportation for providing the funding necessary for improving the pavement response models, performing the calibration of the faulting model and implementing the faulting prediction capabilities into the BCOA-ME. Finally, the authors would like to thank the National Road Research Alliance and the project manager, Mr. John Donohue with the Missouri Department of Transportation, for supporting the development of the climatic models that enabled the capability of the BCOA-ME to predict faulting throughout the United States.

The authors would like to thank Drs. John Harvey and Angel Mateos with the University of California Pavement Research Center for accelerated pavement testing performance data for model validation. Ms. Linda Pierce of NCE was also extremely helpful in providing faulting data collected under NCRHP 1-61 that was used in the calibration. Lastly, the authors would also like to thank Mr. Thomas Burnham and the Minnesota Department of Transportation for providing performance data for model validation from the MnROAD Test Facility. This procedure could not have been developed without the MnROAD performance data. Mr. Burnham was also extremely helpful in providing falling weight deflectometer data collected on the MnROAD sections, which was used for model validation and in obtaining cores to validate the crack deployment prediction methodology.

Introduction

Bonded Concrete Overlay of Asphalt (BCOA) pavements is a robust rehabilitation solution for moderately damaged asphalt pavements, which can increase the service life by 10-20 years if designed and constructed properly. BCOA pavements have become popular because they are relatively simple to construct, and the low thickness of the overlay makes it an economical solution. Moreover, as performance data from more projects becomes available, improved design guides can be developed to further their implementation. Such a design guide would consider a variety of factors, such as the concrete mix design, existing Hot Mix Asphalt (HMA) pavement structure, climate, and traffic.

The bonded concrete overlay of asphalt pavements mechanistic-empirical design guide (BCOA-ME) has been developed to supply a Portland cement concrete (PCC) overlay thickness based on precisely these design inputs. This thickness is determined based on a user-specified maximum allowable percent slabs cracked, and this predicted design thickness is then used to evaluate the predicted faulting at the end of the design period. The fatigue cracking evaluation incorporates field data from broadly three categories of slab sizes: small slabs (slab size < 4.5 ft), medium slabs (slab size between 4.5 ft and 7 ft) and large slabs (slabs longer than 7 ft). The mechanism of development of cracking varies for these sizes, and BCOA-ME incorporates these different mechanisms. The panel size is also limited to no more than 15 ft because smaller slab sizes are needed to get the necessary performance from these thin bonded overlays.

In addition to mechanistic considerations, the design also considers the economy and functionality of the design. Slab thicknesses are limited to 5.5 in for small slabs and 6.5 in for medium and small slabs. Additionally, the thickness of the slab is kept to at least 3.0 in for small and medium slabs, and 4.5 in for large slabs. The thickness of the HMA layer is also restricted to between 3 and 7 in. With thinner HMA layers, insufficient structure is available to strengthen the composite layer, and in that case, it should be treated as a base layer under a new pavement. With an HMA thickness greater than 7 in, the additional structural support has a negligible effect on any added reduction in stress or deflections.

In addition to fatigue damage, faulting has been observed as being the other major distress that can develop in BCOAs. Consequently, BCOA-ME evaluates the predicted faulting using the thickness

recommended by the fatigue cracking model. In this case however, faulting is only estimated for the medium and large slabs as insufficient faulting performance data was available to be able to characterize how faulting develops for the small slab sizes. For large slabs, significant faulting can developed as the joint has been observed to activate through both the PCC and HMA layers, enabling the slab to deflect significantly. For medium sized slabs, only a few of the joints experience full-depth joint activation, while most of the joints propagate only through the overlay. The latter configuration leads to slower development of faulting, and BCOA-ME uses a weighted average of the two joint activation depths while reporting the total faulting for overlays with medium slab sizes.

The purpose of this theory manual is to elaborate on the process and calculations utilized in the design procedure. This manual is subdivided into five sections: 1. traffic, 2. temperature gradient, 3. hot mix asphalt (HMA) modulus, 4. fatigue, and 5. faulting. The inputs need for the design procedure are discussed and the theory behind the design process is presented for each. Sections 1-3 define the inputs common to both the fatigue and faulting analyses (traffic, temperature gradient, and HMA modulus), Section 4 presents the fatigue prediction model, and Section 5 describes the faulting model.

1. Traffic Considerations

In this design procedure, traffic calculations are performed using the concept of 18-kip equivalent single axle loads (ESALs). The equation used for calculating design ESALs is given as:

$$ESAL_{design} = DD \times LDF \times G_f \times ESAL_{daily} \times 365 \quad (1)$$

where,

DD is the directional distribution factor and indicates the fraction of total traffic in the design direction. For one-way traffic, which is required for this procedure, the default value is 1.0.

LDF is the lane distribution factor and is adopted from AASHTO 1993 (p. II-9) as a function of the number of traffic lanes in each direction.

G_f is the traffic growth factor which is calculated using either Equation (2) or Equation (3) depending on the type of growth rate.

$ESALs_{daily}$ is the sum of daily equivalent single axle loads determined for each type of axle load given by Equation (4).

The traffic growth factor for a nonlinear growth rate is given by:

$$G_f = \frac{\left[\left(1 + G_{r,ADTT}\right)^n - 1\right]}{G_{r,ADTT}} \quad (2)$$

The traffic growth factor for a linear growth rate is given by:

$$G_f = n \times \left(1 + G_{r,ADTT} \times \frac{(n-1)}{2}\right) \quad (3)$$

where,

$G_{r,ADTT}$ is the growth rate of average daily truck traffic (ADTT) defined by the user.

n is the design life (years).

The ESALs for a specific type of axle loading is estimated using:

$$ESALs_{daily} = N_R \times LEF \quad (4)$$

where,

N_R is the number of repetitions for a specific axle load per day and can be calculated from Equation (5).

LEF is the load equivalency factor and is calculated through the AASHTO relationship given in Equation (7).

$$N_R = \frac{ADTT}{1000} \times Axles\ per\ 1000\ trucks \tag{5}$$

where,

$Axles\ per\ 1000\ trucks$ information is adopted from the axle load distributions provided in the ACPA guidelines for "Design of Concrete Pavement for City Streets" (2002) and is a function of road category, the axle type, and the axle load, as shown in Table 1.

Table 1: Axles per 1000 trucks for different road categories. Source: "Design of Concrete Pavement for City Streets" (2002).

Axle load (Kips)	Axles per 1000 trucks			
	Category LR	**Category 1**	**Category 2**	**Category 3**
Single axles				
4	846.15	1693.31	0.00	0.00
6	369.97	732.28	0.00	0.00
8	283.13	483.10	233.60	0.00
10	257.60	204.96	142.70	0.00
12	103.40	124.00	116.76	182.02
14	39.07	56.11	47.76	47.73
16	20.87	38.02	23.88	31.82
18	11.57	15.81	16.61	25.15
20	0.00	4.23	6.63	16.33
22	0.00	0.96	2.60	7.85
24	0.00	0.00	1.60	5.21
26	0.00	0.00	0.07	1.78
28	0.00	0.00	0.00	0.85
30	0.00	0.00	0.00	0.45
Tandem axles				
4	15.12	31.90	0.00	0.00
8	39.21	85.59	47.01	0.00
12	48.34	139.30	91.15	0.00
16	72.69	75.02	59.25	99.34
20	64.33	57.10	45.00	85.94
24	42.24	39.18	30.74	72.54
28	38.55	68.48	44.43	121.22
32	27.82	69.59	54.76	103.63
36	14.22	4.19	38.79	56.25
40	0.00	0.00	7.76	21.31
44	0.00	0.00	1.16	8.01
48	0.00	0.00	0.00	2.91
52	0.00	0.00	0.00	1.19

LR = Light residential

ADTT is the average daily truck traffic given as:

$$ADTT = ADT \times Truck\ percent \quad (6)$$

where,

ADT is the user-inputted average daily traffic. If unavailable, ADTT can be estimated based on the typical values of ADTT for different road categories given in Table 2.

$Truck\ percent$ is the percentage of total traffic comprised of trucks. A default value of 6% is provided in the design procedure.

Table 2: ADTT given for different road categories and classifications.

Classification	ADTT	Road category
Light Residential	3	LR
Residential	10 to 50	1
Collector	50 to 500	2
Business	400 to 700	
Minor Arterial	300 to 600	
Industrial	300 to 800	3
Major Arterial	700 to 1500	

The LEF used in Equation (4) can be estimated using the following equation:

$$LEF = \left(\frac{W_x}{W_{18}}\right)^{-1} \tag{7}$$

where,

W_x is the number of 18-kip ESALs for any loading x, and $W_x = W_{18}$ for x = 18 kips. W_x is calculated using the following equation:

$$\text{Log}(W_x) = 5.908 - 4.62\log(L_x + L_2) + 3.28\log(L_2) + \frac{G_t}{\beta_x} - \frac{G_t}{\beta_{18}} \tag{8}$$

where,

L_x is the axle loading, kips.

L_2 is the weight of the axle (1 for single axle and 2 for tandem axle).

β_x is a constant to reflect the current loading in kips, x. $\beta_x = \beta_{18}$ for x = 18 kips. They are given by Equations (9) and (10).

$G_t$is the growth rate and is given by Equation (11).

$$\beta_x = 1 + \frac{3.63(L_x + L_2)^{5.2}}{(h_{PCC} + 1)^{8.46} {L_2}^{3.52}} \tag{9}$$

$$\beta_{18} = 1 + \frac{1.62\ x10^7}{(h_{PCC} + 1)^{8.46}} \tag{10}$$

where,

h_{PCC} is the PCC thickness, in.

$$G_t = \log\left(\frac{4.5 - P_t}{4.5 - 1.5}\right) \quad (11)$$

where,

P_t is the pavement terminal serviceability.

As will be discussed later, cumulative ESALs over the design life (calculated from Equation (1)) is used to predict fatigue cracking in BCOA, while monthly repetitions for each axle load (N_R from Equation (5) is multiplied by 30 before being used in Equation (4)) is used to evaluate monthly and cumulative faulting.

2. Temperature Gradient

The temperature gradient causes the slab to curl and creates an environmental stress in addition to the stress due to traffic loading. In the available structural models for whitetopping slabs, a linear temperature gradient is required to calculate this environmental stress. Since the temperature variation through the slab is nonlinear, an accurate estimate of environmental stress is not possible with the linear temperature gradient. The effective equivalent linear temperature gradient (EELTG) is thus proposed as an input that characterizes the environmental stress.

The framework used to establish the EELTG is illustrated by Figure 1. A database was first populated to produce several whitetopping sites that represent all the climatic conditions in the continental United States, as shown in Figure 2. For each site shown in Figure 2, multiple whitetopping projects representing different structural features, such as PCC overlay thickness, existing asphalt thickness, etc. were simulated. The nonlinear temperature gradient for each project was then obtained on an hourly basis using the Enhanced Integrated Climatic Model (EICM) (Larson and Dempsey, 2003) considering different whitetopping structures. The hourly nonlinear temperature gradients were then converted to hourly equivalent linear temperature gradients (ELTGs) based on strain equivalency. Finally, the EELTG was determined as the equivalent linear temperature gradient that, when applied throughout the design life results in the same amount of damage as if the hourly linear temperature gradients were used. Here, damage can be from fatigue or faulting, and the models described in Sections 4 and 5 respectively are used to evaluate each. Thus, a different EELTG is established for each of the two failure modes (faulting and cracking). Based on the database, a statistical relationship was established between the EELTG and the climatic and structural features of the PCC overlay for both faulting and fatigue. For fatigue, the

relation for the EELTG is expressed separately for three different slab sizes given in Equations (12) through (14). More details regarding establishing this input can be found in (Mu and Vandenbossche, 2012 and DeSantis et. al, In-press). For faulting, the corresponding relations for different slab sizes are given in Equations (15) through (17), the details of which can be found in (DeSantis et al., 2019).

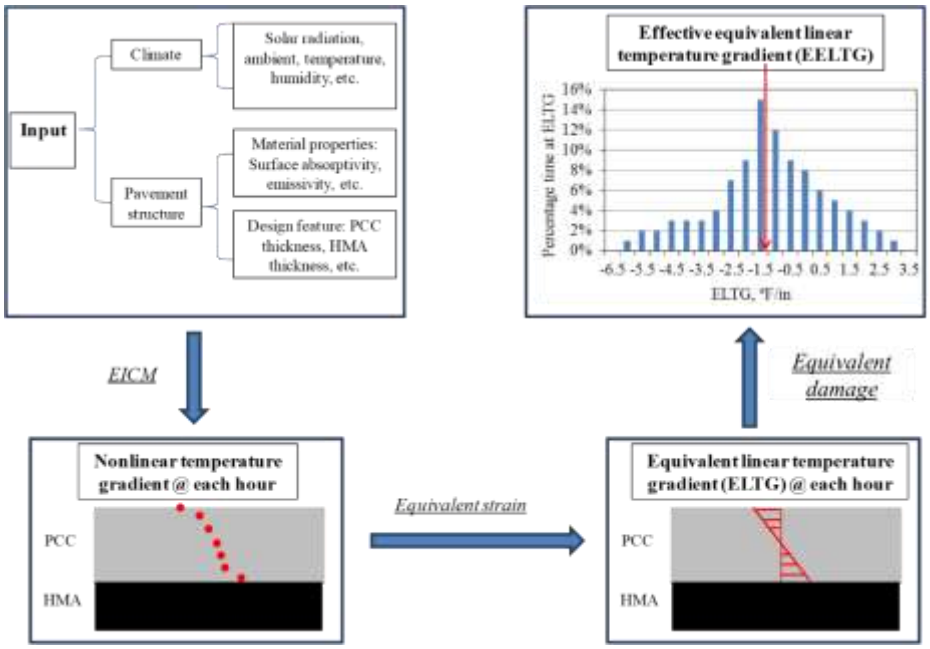

Figure 1: Flowchart to generate the effective equivalent linear temperature gradient.

Figure 2: Whitetopping sites representing all climates of the continental United States (The background map is the Google Map of the US as of June, 2010).

2.1 EELTG for fatigue cracking

For smaller slabs (slabs with a joint spacing ≤ 4.5 ft × 4.5 ft), the $EELTG_{small\ slabs}^{fatigue}$ is given by (R^2 adj = 0.640):

$$EELTG_{small\ slabs}^{fatigue} = 0.534 - 0.0015644Latitude - 0.0009853Longitude - 0.00002145Elevation - 0.0067836S_{ave} + 0.15843L - 0.202627h_{HMA} - 0.00175066M_R \quad (12)$$

For mid-size slabs (slabs with a joint spacing $>$ 4.5 ft and $\leq$ 7 ft), the $EELTG_{mid-size\ slabs}^{fatigue}$ is given by (R^2 adj = 0.710):

$$EELTG_{mid-size\ slabs}^{fatigue} = 0.85895 + 0.0046918\ Latitude + 0.0018581\ Longitude + 0.000003625\ Elevation - 0.0082567\ S_{ave} - 0.127695\ h_{HMA} + 0.00077175\ M_R \quad (13)$$

For larger slabs which span a single lane width, the $EELTG_{large\ slabs}^{fatigue}$ is given by (R^2 adj = 0.480):

$$EELTG_{large\ slabs}^{fatigue} = 2.791 + 0.011843\ Latitude + 0.00134661\ Longitude + 0.0000058\ Elevation + 0.0091791\ S_{ave} - 0.070225\ h_{HMA} + 0.0013025\ M_R - 0.45202\ h_{pcc} \quad (14)$$

where,

$EELTG$ is the effective equivalent linear temperature gradient, °F/in.

$Latitude$ is the geographical latitude of the project location, degrees.

$Longitude$ is the geographical longitude of the project location, degrees.

$Elevation$ is the distance of the project location above sea level, ft.

S_{ave} is the annual mean percentage of sunshine, %.

L is the PCC overlay slab size, ft.

h_{HMA} is the hot mix asphalt (HMA) layer thickness, in.

h_{pcc} is the PCC overlay thickness, in.

M_R is the PCC modulus of rupture, psi.

2.2 EELTG for faulting

Faulting is not evaluated for small-sized slabs (joint spacing $\leq$ 4.5 ft) for reasons previously discussed. For medium-sized slabs (slabs with joint spacing $\leq$ 10 ft), two EELTGs were calculated, one corresponding to joint activation through both the PCC and HMA layers, $EELTG_{Mid-Full}^{faulting}$, and one through only the PCC layer, $EELTG_{Mid-PCC}^{faulting}$. Due to the insensitivity of the shorter slabs, a constant value was found to be sufficient to obtain accurate results:

$$EELTG_{Mid-Full}^{faulting} = -1.5 \quad (15)$$

$$EELTG_{Mid-PCC}^{faulting} = -1.5 \quad (16)$$

For large slabs (slab length > 10 ft), where the joint always activates through both the PCC and HMA layers, $EELTG_{Large-Full}^{faulting}$ is shown below (R^2 adj = 0.731):

$$EELTG_{Large-Full}^{faulting} = 10.46 - 1.17\,L - 0.0033\,LTEshoulder - 6.85E\text{-}07\,E_{PCC} - 1.14\,Dowel\_diam - 0.36\,h_{PCC} - 0.35\,h_{HMA} + 0.01\,AMDAT - 0.031\,Latitude + 0.0038\,Longitude - 0.0002\,Elevation - 0.0013\,S_{ave} + 0.0006\,L*LTEshoulder + 9.06E\text{-}08\,L*E_{PCC} + 0.11\,L*Dowel\_diam + 0.05\,L*h_{PCC} - 0.0046\,L*h_{HMA} + 0.0008\,L*Longitude + 9.57E\text{-}06\,L*Elevation + 0.0006\,L*S_{ave} - 1.32E\text{-}09\,LTEshoulder*E_{PCC} + 0.0015\,LTEshoulder*Dowel\_diam - 0.0004\,LTEshoulder*h_{PCC} + 0.0005\,LTEshoulder*h_{HMA} - 3.01E\text{-}05\,LTEshoulder*Latitude + 5.03E\text{-}06\,LTEshoulder*Longitude + 2.44E\text{-}08\,E_{PCC}*Dowel\_diam - 3.91E\text{-}08\,E_{PCC}*h_{PCC} + 2.47E\text{-}08\,E_{PCC}*h_{HMA} - 9.68E\text{-}10\,E_{PCC}*AMDAT - 1.39E\text{-}09\,E_{PCC}*S_{ave} - 0.06\,Dowel\_diam*h_{PCC} + 0.03\,Dowel\_diam*h_{HMA} - 0.0007\,Dowel\_diam*AMDAT - 0.0010\,Dowel\_diam*Longitude + 0.0276\,h_{PCC}*h_{HMA} - 0.0022\,h_{PCC}*Latitude - 0.0003\,h_{HMA}*Longitude + 1.25E\text{-}06\,h_{HMA}*Elevation + 0.0009\,h_{HMA}*S_{ave} - 0.0001\,AMDAT*Longitude + 1.02E\text{-}06\,AMDAT*Elevation - 0.0001\,Longitude*S_{ave} + 3.44E\text{-}07\,Elevation*S_{ave} + 0.0056\,h_{HMA}*h_{HMA} + 0.0005\,Latitude*Latitude \quad (17)$$

where,

LTEshoulder is the load transfer efficiency between the slab and the shoulder, %.

E_{PCC} is the modulus of the overlay, psi

Dowel_diam is the diameter of the dowel bars used, in.

AMDAT is the mid-value of the AMDAT that corresponds to the AMDAT Zone discussed in Section 2.3, °F.

Longitude is the absolute value of the longitude of the location, degrees.

The units of each of the EELTG's is °F/in. $EELTG_{Large-Full}^{faulting}$ is further limited to values between 0.0 and -3.0 °F/in.

2.3 Determination of Inputs for EELTG

The calculation of EELTG requires user-defined geographic inputs including latitude, longitude, and elevation, as well as user-defined structural design inputs including the PCC overlay slab size, HMA layer thickness, and the PCC modulus of rupture. Additionally, the annual mean percentage of sunshine (S_{ave}) is also required and typical values based on geographic zones are given in Figure 3.

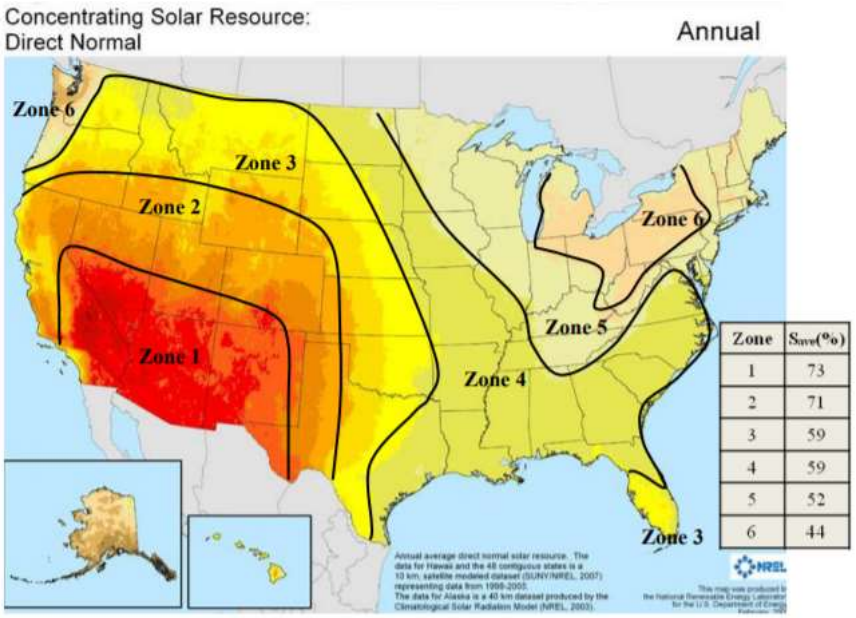

Figure 3: Zonal division of the US in terms of the annual mean percentage of sunshine (based on the annual concentrating solar resource map of the US in 2009, http://www.nrel.gov/gis/solar.html).

Seasonal temperature variations across the country are also taken into consideration for some of the inputs. To simplify this input, seven temperature regions were established based on the annual mean daily average temperature (AMDAT) map as shown in Figure 4.

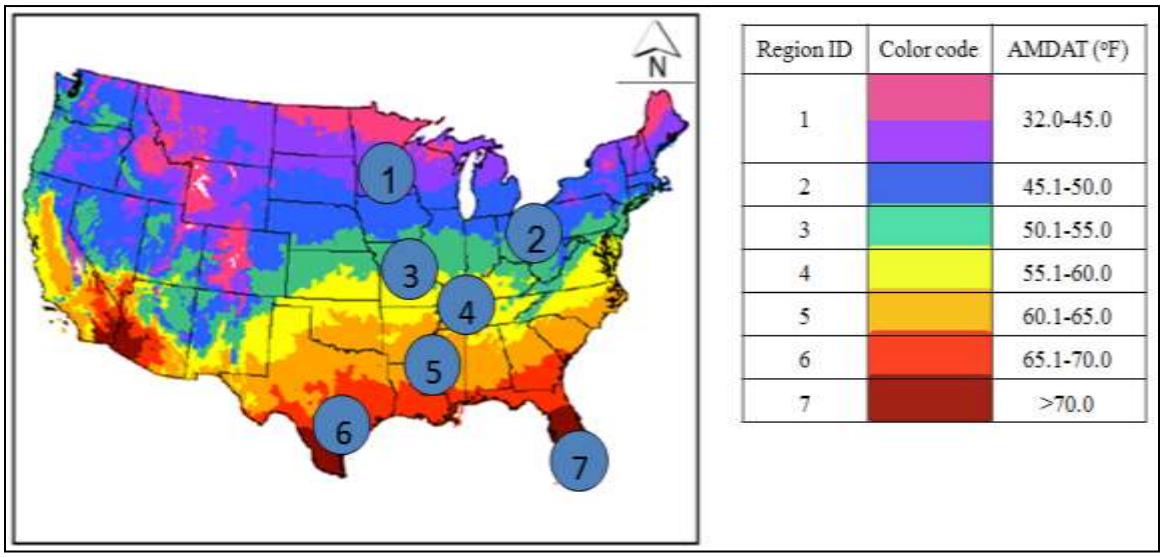

Region ID	Color code	AMDAT (°F)
1		32.0-45.0
2		45.1-50.0
3		50.1-55.0
4		55.1-60.0
5		60.1-65.0
6		65.1-70.0
7		>70.0

Figure 4: Regional division of the US in terms of the annual mean daily average temperature (AMDAT) (http://cdo.ncdc.noaa.gov/climaps/temp0313).

2.4 Additional Inputs Extracted from EICM Data

In addition to EELTG, three other parameters were determined using output from EICM. They include WETDAYS, Freezing Ratio (FR), and mean monthly nighttime mid-depth PCC temperature. These parameters are used in the faulting prediction model, as discussed in Section 5. WETDAYS is defined as the average number of days in a year with precipitation greater than 0.1 in, and is important as moisture contributes to the development of pumping (and hence faulting). The freezing ratio is defined as the percentage of time that the top of the base layer or asphalt layer, depending on full- or partial-depth joint activation respectively, is less than 32 ^{o}F (freezing temperature). The significance of this variable is to be able to know how often the base or asphalt layer is frozen. The erodibility of the is reduced when the material is frozen, and therefore the development of faulting.

Based on data from the locations identified in Figure 2, the following regression equations were developed and implemented for WETDAYS (R^2 adj = 0.590) and FR:

$$WETDAYS = -102.3 + 25.81 bSunZone + 2.063\ AMDATZone - 1.216\ Latitude + 0.3804\ Longitude + 1.429\ S_{ave} \quad (18)$$

$$FR = C_1 + C_2\ h_{PCC} + C_3\ h_{HMA} + C_4\ AMDATZone + C_5\ Latitude + C_6\ Longitude + C_7\ Elevation \quad (19)$$

Where,

SunZone is the sunshine zone of the project location, as shown in Figure 3.

AMDATZone is the AMDAT zone shown in Figure 4.

The coefficients $C_1 - C_7$ in Equation (19) are functions of the sunshine zone and are shown in Table 3.

Table 3: Freezing ratio regression coefficients.

Sun. zone	C_1	C_2	C_3	C_4	C_5	C_6	C_7	**R^2 adj.**
PCC-depth joint activation								
1	-87.1	-0.111	-0.140	-2.58	0.711	0.705	4.2E-04	0.699
2	73.21	-0.094	-0.281	-7.332	0.878	-0.551	-3.5E-03	0.607
3	80.4	-0.008	-0.136	-5.342	0.096	-0.563	7.4E-04	0.686
4	-53.71	-0.004	-0.106	-3.141	0.864	0.502	3.1E-03	0.920
5	-77.15	0.066	-0.218	-1.763	1.998	0.149	1.9E-03	0.922
6	-15.74	-0.017	-0.255	-2.072	1.821	-0.495	9.4E-04	0.840
Full-depth joint activation								
1	-146.78	-0.133	-0.324	-3.102	0.446	1.333	1.5E-03	0.680
2	84.51	-0.172	-0.770	-7.767	1.419	-0.776	4.0E-03	0.536
3	32.731	-0.030	-0.137	-5.659	0.072	-0.024	2.2E-04	0.697
4	32.731	-0.030	-0.137	-5.659	0.072	-0.024	2.2E-04	0.697
5	81.919	-0.010	-0.083	-7.967	-0.472	-0.302	3.6E-03	0.698
6	52.531	-0.247	0.003	-4.036	-0.940	0.217	-3.1E-03	0.636

The mean mid-depth temperature is evaluated as the product of a reference temperature (in January) and a monthly adjusted factor. The reference temperature is shown in Equation (20) below, with R^2 adj = 0.810.

$$T_{mid-depth(Ref)} = 58.72 - 0.123h_{PCC} - 1.455SunZone + 5.817AMDATZone - 0.67Latitude + 0.2429\ Longitude + 0.00104\ Elevation - 0.584\ S_{ave} \quad (20)$$

Adjustment factors are shown in Table 4.

Table 4: Mean monthly nighttime PCC mid-depth temperature adjustment factors.

AMDAT zone	$T_{mid-depth(Ref)}$, **°F (Avg./Std. dev.)**	**Adjustment factor for each month**											
		Jan	**Feb**	**Mar**	**Apr**	**May**	**Jun**	**Jul**	**Aug**	**Sep**	**Oct**	**Nov**	**Dec**
1	21.62	1.0	1.0	1.8	2.7	3.6	4.1	4.6	4.6	3.8	2.8	2.3	1.2
	7.65	0.0	1.2	4.8	7.8	11.1	13.9	16.8	16.4	13.5	8.2	5.9	0.3
2	29.44	1.0	1.1	1.4	2.0	2.5	2.9	3.1	3.1	2.6	2.1	1.8	1.3
	5.05	0.0	0.1	0.1	0.4	0.4	0.5	0.5	0.5	0.4	0.3	0.3	0.3
3	33.53	1.0	1.2	1.4	2.0	2.4	2.6	2.8	2.8	2.4	1.9	1.7	1.3
	5.48	0.0	0.1	0.2	0.3	0.4	0.4	0.5	0.5	0.4	0.3	0.2	0.2
4	39.67	1.0	1.2	1.4	1.8	2.1	2.4	2.5	2.5	2.2	1.8	1.6	1.3
	7.86	0.0	0.1	0.1	0.3	0.3	0.4	0.4	0.4	0.3	0.2	0.2	0.1
5	47.79	1.0	1.2	1.3	1.6	1.9	2.0	2.1	2.1	1.9	1.6	1.4	1.2
	4.97	0.0	0.1	0.1	0.1	0.1	0.2	0.2	0.2	0.2	0.1	0.1	0.1
6	53.62	1.0	1.2	1.3	1.5	1.7	1.8	1.9	1.9	1.7	1.5	1.3	1.1
	4.54	0.0	0.1	0.1	0.1	0.2	0.2	0.2	0.2	0.2	0.1	0.1	0.1
7	67.69	1.0	1.1	1.2	1.3	1.4	1.5	1.5	1.6	1.5	1.3	1.2	1.1
	8.24	0.0	0.0	0.1	0.1	0.2	0.2	0.2	0.2	0.2	0.1	0.1	0.1

3. Characterization of the HMA Modulus

The HMA modulus changes directly with seasonal and daily temperature variations; however, in previous design procedures, a constant HMA modulus is used. This assumption predicts uniform fatigue or faulting consumption throughout the year while accounting for the increased fatigue or faulting consumption that occurs during the summer months. In this design procedure, the HMA modulus adjustment factors are used to adjust the reference month HMA modulus that account for both the seasonal and hourly variation of the HMA modulus on the fatigue or faulting of the overlay.

An investigation was carried out to determine the factors affecting the temperature related HMA modulus fluctuation. This investigation revealed that the time of year (season) and the geographic location of the project were the two primary factors influencing the HMA modulus fluctuation, both of which were characterized using the AMDAT zone.

3.1 Considerations in Establishing Effective HMA Modulus Values

The framework used to establish the HMA asphalt stiffness adjustment factor (F) for the seven different temperature regions is shown in Figure 5(a) for the fatigue analysis and Figure 5(b) for the faulting analysis. For every weather station in each region, monthly HMA temperature is first estimated using the Enhanced Integrated Climatic Model (EICM). The same database of weather stations used for the EELTG analysis, as shown in Figure 2, was selected. Then, using the master curve (ARA, 2004) the HMA modulus for different temperatures was determined for each region. A uniform aggregate gradation was chosen for all regions. SHRP LTPP BIND version 3.1 (Pavement System LLC, 2005), which is a Superpave binder selection program developed for the Federal Highway Administration (FWHA), was used to choose asphalt binder grade according to the location of the project for each zone. Then, the hourly and monthly HMA modulus for each weather station was determined using the corresponding hourly and monthly mean temperature of the region.

The fatigue accumulation using the hourly HMA modulus for a certain month is denoted as FA_h, while the fatigue accumulation using the monthly HMA modulus for the same month is FA_m. The difference between FA_h and FA_m indicates the effect of hourly HMA modulus variation and it is a function of design features and material properties. A large number of hypothetical designs are

considered for the fatigue analysis. The design variables considered in the fatigue analysis can be found in Table 3(a).

Similarly, faulting damage is expressed in terms of differential energy (discussed in detail in Section 5). The differential energy determined using the hourly HMA modulus for a certain month is denoted as DE_h, while the differential energy determined using the monthly HMA modulus for the same month is DE_m. The monthly HMA modulus is adjusted until the two differential energies are equal for several hypothetical designs. The design variables considered in the fatigue analysis can be found in Table 3(b).

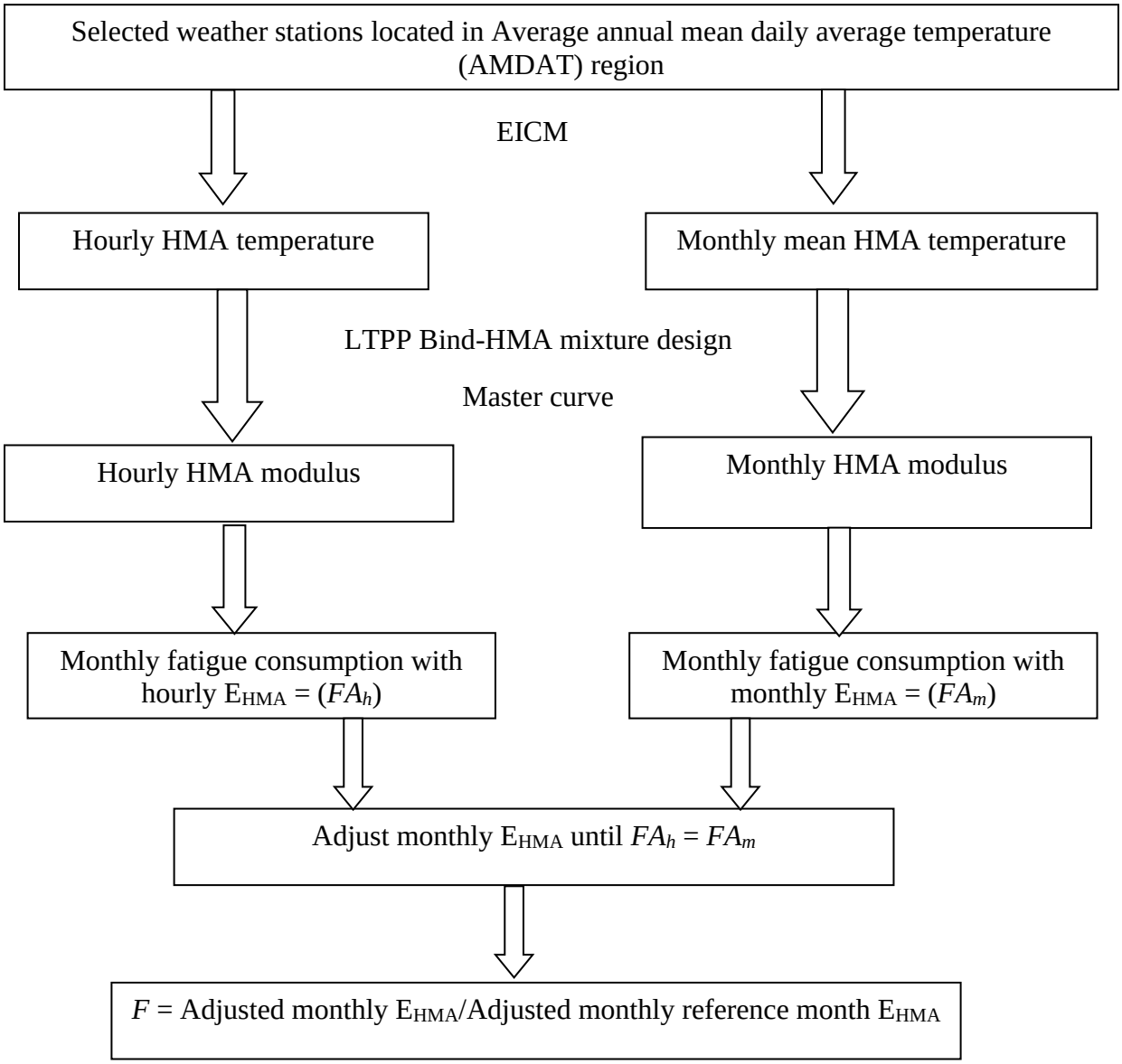
Selected weather stations located in Average annual mean daily average temperature (AMDAT) region
EICM
Hourly HMA temperature
Monthly mean HMA temperature
LTPP Bind-HMA mixture design
Master curve
Hourly HMA modulus
Monthly HMA modulus
Monthly fatigue consumption with hourly E_{HMA} = (FA_h)
Monthly fatigue consumption with monthly E_{HMA} = (FA_m)
Adjust monthly E_{HMA} until $FA_h = FA_m$
F = Adjusted monthly E_{HMA}/Adjusted monthly reference month E_{HMA}

(a)

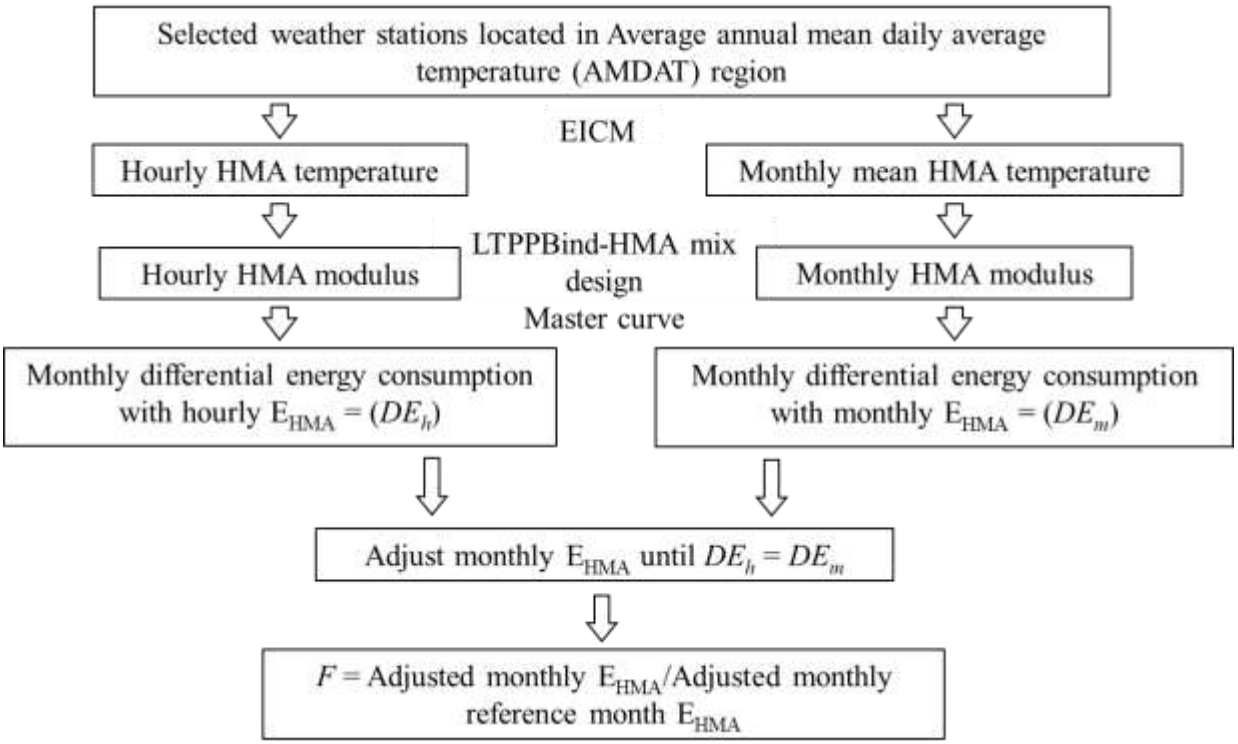

(b)

Figure 5: Framework for establishing the effective HMA modulus adjustment factor, (*F*) for (a) fatigue analysis and (b) faulting analysis.

Table 3: Whitetopping design features and material properties considered in the (a) fatigue analysis and (b) faulting analysis.

(a) Design features in the fatigue analysis			
Joint spacing	**PCC layer thickness (in)**	**HMA layer thickness (in)**	**Panel size (ft ×ft)**
≤4.5 ft	3 and 4	4 and 8	3 × 3 and 4 × 4
>4.5 ft ≤ 7 ft	3, 4, and 6	4 and 8	6 × 6
> 7 ft	5 and 6	4, 6, and 8	10 × 12

Material properties					
Concrete MOR (psi)	**PCC modulus (10^6 psi)**	**Concrete CTE ($10^{-6}/^0$F)**	**k (pci)**	**Poisson's ratio of PCC**	**Poisson's ratio of HMA**
550, 650 and 750	3.5, 4, 4.4	5	200	0.15	0.35

(b) Design features in the faulting analysis		
	Joint spacing (ft)	
	< 10	≥ 10
PCC layer thickness (in)	3, 4, and 6	5 and 6
Asphalt layer thickness (in)	4 and 8	4, 6, and 8
Joint spacing (ft)	6 x 6 8 x 8	10 x 12 12 x 12
Joint activation depth	PCC only Full-depth	Full-depth
PCC MOR (psi)	550, 650, and 750	
PCC modulus (10^6 psi)	3.5, 4.0, and 4.5	
Dowel diameter (in)	0 and 1.25	
PCC CTE ($10^{-6}/^o$F)	5.0	
k-value (psi/in)	200	
Poisson's ratio of PCC	0.18	
Poisson's ratio of asphalt	0.35	

For each design at a certain location, there are twelve effective monthly HMA modulus values, which were normalized to a reference month, defined as the HMA modulus adjustment factors ($F_{fatigue}$ and $F_{faulting}$). Regression models are then developed for predicting the adjustment factors as a function of HMA thickness and normalized mid-depth HMA temperature, as demonstrated in Equation (21) for fatigue cracking and (22) for faulting. These equations reflect the change in the HMA modulus as a function of seasonable and hourly temperature variation. As

shown in Figure 4, the seasonal temperature variation across the country can be subdivided into seven temperature regions according to the annual mean daily average temperature (AMDAT). For fatigue cracking, three different design approaches are used based upon failure mode, which is dictated by the slab size. This results of the three sets of values for the regression coefficients in Equation (21) are given with, the respective R^2 values in Table 4(a). Similarly, for faulting, the coefficients in Equation (22) for three different damage models, which are based on slab size (medium and large slabs only) and depth of joint activation, are shown in Table 4(b).

$$F_{fatigue} = C_1 + \frac{C_2}{T_{norm}} + C_3\, h_{HMA} + C_4\, h_{PCC} \tag{21}$$

$$F_{faulting} = \sum(Terms \times Coefficients) \tag{22}$$

where,

F is the HMA modulus adjustment factor that accounts for seasonal variation of the HMA modulus (fatigue or faulting as denoted by the subscript) and the effect of the hourly temperature variation on the fatigue of the overlay.

T_{norm} is normalized mid-depth HMA temperature of the project location.

Table 4: HMA modulus adjustment factor coefficients by zone for (a) fatigue analysis and (b) faulting analysis.

(a) Fatigue Analysis							
≤ 4.5 ft × 4.5 ft joint spacing	**Zone 1**	**Zone 2**	**Zone 3**	**Zone 4**	**Zone 5**	**Zone 6**	**Zone 7**
C_1	-0.139	-0.246	-0.300	-0.310	-0.525	-0.654	-0.428
C_2	1.07	1.25	1.32	1.31	1.51	1.66	1.41
C_3	-0.00576	-0.00657	-0.00804	-0.00764	-0.00335	-0.00540	-0.00705
C_4	0	0	0	0	0	0	0
R^2	0.871	0.913	0.892	0.897	0.925	0.944	0.868
> 4.5 ft and ≤ 7 ft joint spacing	**Zone 1**	**Zone 2**	**Zone 3**	**Zone 4**	**Zone 5**	**Zone 6**	**Zone 7**
C_1	-0.2169	-0.3455	-0.4058	-0.3747	-0.4566	-0.4726	-0.4968
C_2	1.05296	1.1836	1.2773	1.2575	1.4604	1.5751	1.4385
C_3	0.00581	0.00801	0.00434	-0.000016	-0.007	-0.0129	-0.0025
C_4	0.008295	0.0145	0.01658	0.01371	0.00202	-0.0107	0.00429
R^2	0.857	0.798	0.881	0.870	0.912	0.940	0.862
> 7 ft transverse joint spacing	**Zone 1**	**Zone 2**	**Zone 3**	**Zone 4**	**Zone 5**	**Zone 6**	**Zone 7**
C_1	0.09321	0.02420	0.11736	-0.0688	-0.2431	-0.0635	-0.0950
C_2	0.76515	0.85253	0.71162	0.92720	1.0960	0.8516	0.9290
C_3	0.01936	0.025210	0.02728	0.02867	0.02822	0.02641	0.02136
C_4	0	0	0	0	0	0	0
R^2	0.659	0.641	0.563	0.615	0.613	0.652	0.683

(b) Faulting Analysis					
Joint spacing < 10 ft with joint activation through PCC only					
AMDAT Zone = 1		**AMDAT Zone = 2**		**AMDAT Zone = 3**	
Term	**Coefficient**	**Term**	**Coefficient**	**Term**	**Coefficient**
(Intercept)	6.17E+01	*(Intercept)*	2.54E+00	*(Intercept)*	-1.10E+01
L	1.40E+00	*L*	1.01E+00	*L*	1.04E+00
h_{PCC}	1.75E+00	h_{PCC}	1.97E+00	h_{PCC}	2.45E+00

h_{HMA}	-6.46E-01	h_{HMA}	-1.03E+00	h_{HMA}	-7.33E-01
S_{ave}	4.29E-01	S_{ave}	-8.03E-03	S_{ave}	1.40E-01
Latitude	-3.25E+00	*Latitude*	-2.20E-01	*Latitude*	3.00E-02
Longitude	-8.44E-02	*Longitude*	-8.15E-02	*Longitude*	-3.81E-03
Elevation	-2.05E-03	*Elevation*	4.25E-04	*Elevation*	-6.56E-04
T_{norm}	1.27E+00	T_{norm}	3.38E+00	T_{norm}	1.85E+00
$L^* h_{PCC}$	-1.99E-01	$L^* h_{PCC}$	-1.71E-01	$L^* h_{PCC}$	-1.92E-01
L^*h_{HMA}	-1.36E-02	*L*Longitude*	1.20E-03	*L*P_Sunshine*	3.09E-03
L^*T_{norm}	-2.07E-01	L^*T_{norm}	-1.84E-01	L^*T_{norm}	-1.61E-01
$h_{PCC}*h_{HMA}$	-2.83E-02	$h_{PCC}*h_{HMA}$	-3.75E-02	$h_{PCC}*h_{HMA}$	-5.92E-02
$h_{PCC}*T_{norm}$	-1.67E-01	$h_{PCC}*S_{ave}$	-2.17E-03	$h_{PCC}*S_{ave}$	-6.44E-03
h_{HMA}*Latitude	9.43E-03	$h_{PCC}*T_{norm}$	-3.78E-01	$h_{PCC}*T_{norm}$	-3.47E-01
h_{HMA}*Elevation	1.70E-05	h_{HMA}*Latitude	1.84E-02	$h_{HMA} * S_{ave}$	1.91E-03
$h_{HMA}*T_{norm}$	8.31E-02	h_{HMA} *Longitude	-1.53E-03	h_{HMA} *Latitude	1.20E-02
S_{ave}*Latitude	5.77E-03	h_{HMA} *Elevation	3.51E-05	h_{HMA} *Longitude	-2.22E-03
S_{ave} *Longitude	1.30E-02	$h_{HMA} *T_{norm}$	6.79E-02	h_{HMA} *Elevation	2.36E-05
S_{ave} *Elevation	4.23E-05	S_{ave} *Longitude	2.08E-03	$h_{HMA} *T_{norm}$	1.28E-01
$S_{ave} *T_{norm}$	2.56E-02	S_{ave} *Elevation	-6.00E-06	S_{ave} *Elevation	7.43E-06
*Latitude*Longitude*	-1.34E-02	$S_{ave} *T_{norm}$	4.54E-02	$S_{ave} *T_{norm}$	-2.45E-02
*Latitude*Elevation*	6.60E-05	*Latitude*Longitude*	1.55E-03	*Latitude*T_{norm}*	-1.09E-01
LatitudeT_{norm}*	-1.27E-01	*Latitude*T_{norm}*	-1.60E-01	*Longitude*Elevation*	5.17E-06
*Longitude*Elevation*	-2.99E-05	*Elevation*T_{norm}*	-5.12E-04	*Longitude*T_{norm}*	1.55E-02
LongitudeT_{norm}*	1.16E-02	h_{HMA}^2	3.65E-02	*Elevation*T_{norm}*	-2.77E-04
ElevationT_{norm}*	-3.54E-04	S_{ave}^2	-1.86E-03	h_{HMA}^2	4.09E-02
h_{HMA}^2	2.82E-02	*Latitude*^{2}	1.46E-03	S_{ave}^2	-1.14E-03
S_{ave}^2	-1.80E-02	*Longitude*^{2}	-5.14E-04	*Elevation*^{2}	-3.30E-08
Latitude^2	4.55E-02	*Elevation*^{2}	4.18E-08	T_{norm}^2	1.44E+00
Elevation^2	-2.42E-08	T_{norm}^2	1.34E+00	R^2 adj	0.798
T_{norm}^2	1.03E+00	R^2 adj	0.795		
R^2 adj	0.8				
AMDAT Zone = 4		**AMDAT Zone = 5**		**AMDAT Zone = 6**	
Term	**Coefficient**	**Term**	**Coefficient**	**Term**	**Coefficient**
(Intercept)	1.95E+01	*(Intercept)*	-2.15E+01	*(Intercept)*	1.58E+00
L	1.03E+00	*L*	9.59E-01	*L*	5.06E-01
h_{PCC}	2.52E+00	h_{PCC}	1.31E+00	h_{PCC}	1.00E+00
h_{HMA}	-3.86E-01	h_{HMA}	4.25E-02	h_{HMA}	2.16E-01
S_{ave}	2.32E-01	S_{ave}	4.59E-01	S_{ave}	-6.32E-01
Latitude	-1.52E+00	*Latitude*	5.46E-01	*Longitude*	-3.18E-03
Longitude	-1.05E-01	*Longitude*	-1.46E-01	T_{norm}	1.33E+01
Elevation	-6.49E-04	*Elevation*	6.09E-04	$L^* h_{PCC}$	-7.64E-02
T_{norm}	-4.22E-02	T_{norm}	1.20E+00	*L*Longitude*	-2.17E-03

$L^* h_{PCC}$	-2.01E-01	$L^* h_{PCC}$	-1.27E-01	L^*T_{norm}	1.29E-01
$L^* S_{ave}$	4.55E-03	*L*HHMA*	1.53E-02	$h_{PCC} * h_{HMA}$	-6.22E-02
*L*Tnorm*	-2.12E-01	*L*Latitude*	-7.67E-03	h_{PCC}**Longitude*	4.35E-03
$h_{PCC} * h_{HMA}$	-5.41E-02	L^*T_{norm}	-9.20E-02	h_{PCC} **Tnorm*	-5.31E-01
$h_{PCC} * S_{ave}$	-7.49E-03	$h_{PCC} * h_{HMA}$	-4.92E-02	h_{HMA}**Latitude*	6.60E-03
h_{PCC} **T_{norm}*	-3.19E-01	h_{PCC}**Latitude*	1.34E-02	h_{HMA} **T_{norm}*	-8.32E-02
$h_{HMA} * S_{ave}$	2.50E-03	h_{PCC}**T_{norm}*	-5.88E-01	*Latitude*T_{norm}*	-4.64E-01
h_{HMA} **Elevation*	1.13E-05	h_{HMA}**Longitude*	1.28E-03	*Latitude*^{2}	1.60E-02
h_{HMA} **T_{norm}*	9.50E-02	S_{ave} **Longitude*	-5.44E-03	R^2 adj	0.849
S_{ave} **Elevation*	1.32E-05	S_{ave} **Elevation*	2.54E-05		
S_{ave} **Tnorm*	-4.30E-02	S_{ave} **T_{norm}*	2.40E-02		
*Latitude*Longitude*	1.25E-03	*Latitude*Longitude*	2.60E-03		
ElevationT_{norm}*	-2.66E-04	*Latitude*Elevation*	-2.80E-05		
h_{HMA} ^{2}	3.36E-02	*Latitude*T_{norm}*	-7.05E-02		
S_{ave} ^{2}	-1.85E-03	*Longitude*Elevation*	-1.34E-05		
Latitude^2	1.86E-02	*Longitude* T_{norm}*	-2.14E-02		
Longitude^2	3.63E-04	*Elevation* T_{norm}*	-1.23E-04		
T_{norm}^2	1.63E+00	*Latitude*^{2}	-1.12E-02		
R^2 adj	0.789	*Longitude*^{2}	2.25E-03		
		Elevation^2	4.25E-08		
		T_{norm}^2	1.44E+00		
		R^2 adj	0.768		

AMDAT Zone = 7

Term	**Coefficient**
(Intercept)	-4.38E+02
L	-8.27E-02
h_{PCC}	5.85E-01
h_{HMA}	2.87E-01
S_{ave}	7.76E+00
Latitude	1.24E+01
Longitude	-5.97E-02
Elevation	8.72E-04
T_{norm}	6.39E+00
L^*h_{HMA}	1.35E-02
$h_{PCC} * h_{HMA}$	-4.28E-02
h_{PCC}**T_{norm}*	-3.42E-01
h_{HMA}**T_{norm}*	-1.34E-01
S_{ave} **Latitude*	-2.19E-01
S_{ave} **Tnorm*	-4.58E-01
LatitudeT_{norm}*	5.17E-01
LongitudeT_{norm}*	7.36E-02

ElevationT_{norm}*	-9.08E-04				
R^2 adj	0.81				
Joint spacing < 10 ft with joint activation through both PCC and HMA					
AMDAT Zone = 1		**AMDAT Zone = 2**		**AMDAT Zone = 3**	
Term	**Coefficient**	**Term**	**Coefficient**	**Term**	**Coefficient**
(Intercept)	6.17E+01	*(Intercept)*	2.54E+00	*(Intercept)*	-8.86E+00
L	1.40E+00	*L*	1.01E+00	*L*	1.04E+00
h_{PCC}	1.75E+00	h_{PCC}	1.97E+00	h_{PCC}	2.46E+00
h_{HMA}	-6.46E-01	h_{HMA}	-1.03E+00	h_{HMA}	-7.34E-01
S_{ave}	4.29E-01	S_{ave}	-8.21E-03	S_{ave}	9.13E-02
Latitude	-3.25E+00	*Latitude*	-2.20E-01	*Latitude*	-2.87E-02
Longitude	-8.44E-02	*Longitude*	-8.15E-02	*Longitude*	-4.01E-03
Elevation	-2.05E-03	*Elevation*	4.25E-04	*Elevation*	-2.37E-04
T_{norm}	1.27E+00	T_{norm}	3.38E+00	T_{norm}	1.82E+00
Lh_{PCC}*	-1.99E-01	*L*h_{PCC}*	-1.71E-01	*L*h_{PCC}*	-1.92E-01
Lh_{HMA}*	-1.36E-02	*L*Longitude*	1.20E-03	*L*S_{ave}*	3.09E-03
LT_{norm}*	-2.07E-01	*L*T_{norm}*	-1.84E-01	*L*T_{norm}*	-1.61E-01
h_{PCC}*h_{HMA}	-2.83E-02	h_{PCC}*h_{HMA}	-3.74E-02	h_{PCC}*h_{HMA}	-5.91E-02
h_{PCC}*T_{norm}	-1.67E-01	h_{PCC}*S_{ave}	-2.17E-03	h_{PCC}*S_{ave}	-6.44E-03
h_{HMA}*Latitude	9.43E-03	h_{PCC}*T_{norm}	-3.78E-01	h_{PCC}*T_{norm}	-3.48E-01
h_{HMA} *Elevation	1.70E-05	h_{HMA} *Latitude	1.84E-02	h_{HMA} * S_{ave}	1.90E-03
h_{HMA} *T_{norm}	8.31E-02	h_{HMA} *Longitude	-1.53E-03	h_{HMA} *Latitude	1.20E-02
S_{ave}*Latitude	5.77E-03	h_{HMA} *Elevation	3.51E-05	h_{HMA} *Longitude	-2.22E-03
S_{ave} *Longitude	1.30E-02	h_{HMA} * T_{norm}	6.80E-02	h_{HMA} *Elevation	2.36E-05
S_{ave} *Elevation	4.23E-05	S_{ave} *Longitude	2.08E-03	h_{HMA} *T_{norm}	1.28E-01
S_{ave} * T_{norm}	2.56E-02	S_{ave} *Elevation	-6.02E-06	S_{ave} *Latitude	1.39E-03
*Latitude*Longitude*	-1.34E-02	S_{ave} * T_{norm}	4.54E-02	S_{ave} *Elevation	6.97E-06
*Latitude*Elevation*	6.60E-05	*Latitude*Longitude*	1.55E-03	S_{ave} *T_{norm}	-2.42E-02
Latitude T_{norm}*	-1.27E-01	*Latitude* T_{norm}*	-1.60E-01	*Latitude*Elevation*	-1.21E-05
*Longitude*Elevation*	-2.99E-05	*Elevation* T_{norm}*	-5.12E-04	*Latitude*T_{norm}*	-1.09E-01
Longitude T_{norm}*	1.16E-02	h_{HMA}^2	3.65E-02	*Longitude*Elevation*	6.47E-06
Elevation T_{norm}*	-3.54E-04	S_{ave}^2	-1.86E-03	*Longitude* T_{norm}*	1.55E-02
h_{HMA}^2	2.82E-02	*Latitude*^{2}	1.46E-03	*Elevation* T_{norm}*	-2.78E-04
S_{ave}^2	-1.80E-02	*Longitude*^{2}	-5.14E-04	h_{HMA}^2	4.09E-02
Latitude^2	4.55E-02	*Elevation*^{2}	4.19E-08	S_{ave}^2	-1.22E-03
Elevation^2	-2.42E-08	T_{norm}^2	1.34E+00	*Elevation*^{2}	-4.10E-08
T_{norm}^2	1.03E+00	R^2 adj	0.795	T_{norm}^2	1.43E+00
R^2 adj	0.8			R^2 adj	0.798
AMDAT Zone = 4		**AMDAT Zone = 5**		**AMDAT Zone = 6**	
Term	**Coefficient**	**Term**	**Coefficient**	**Term**	**Coefficient**
(Intercept)	1.95E+01	*(Intercept)*	-2.16E+01	*(Intercept)*	1.58E+00

L	1.03E+00	L	9.60E-01	L	5.06E-01
h_{PCC}	2.52E+00	h_{PCC}	1.31E+00	h_{PCC}	1.00E+00
h_{HMA}	-3.86E-01	h_{HMA}	4.36E-02	h_{HMA}	2.16E-01
S_{ave}	2.32E-01	S_{ave}	4.61E-01	S_{ave}	-6.32E-01
Latitude	-1.52E+00	*Latitude*	5.46E-01	*Longitude*	-3.18E-03
Longitude	-1.05E-01	*Longitude*	-1.45E-01	T_{norm}	1.33E+01
Elevation	-6.49E-04	*Elevation*	6.06E-04	$L*h_{PCC}$	-7.64E-02
T_{norm}	-4.18E-02	T_{norm}	1.22E+00	*L*Longitude*	-2.17E-03
$L*h_{PCC}$	-2.01E-01	$L*h_{PCC}$	-1.27E-01	$L*T_{norm}$	1.29E-01
$L*S_{ave}$	4.55E-03	$L*h_{HMA}$	1.53E-02	$h_{PCC}*h_{HMA}$	-6.22E-02
$L*T_{norm}$	-2.12E-01	*L*Latitude*	-7.67E-03	h_{PCC}*Longitude	4.35E-03
$h_{PCC}*h_{HMA}$	-5.41E-02	$L*T_{norm}$	-9.25E-02	$h_{PCC} *T_{norm}$	-5.31E-01
$h_{PCC} * S_{ave}$	-7.49E-03	$h_{PCC}*h_{HMA}$	-4.93E-02	h_{HMA}*Latitude	6.60E-03
h_{PCC} *Tnorm	-3.19E-01	h_{PCC} *Latitude	1.33E-02	$h_{HMA} *T_{norm}$	-8.32E-02
$h_{HMA} * S_{ave}$	2.50E-03	$h_{PCC} *T_{norm}$	-5.89E-01	*Latitude*T_{norm}*	-4.64E-01
h_{HMA} *Elevation	1.13E-05	h_{HMA} *Longitude	1.28E-03	$Latitude^2$	1.60E-02
$h_{HMA} *T_{norm}$	9.50E-02	S_{ave} *Longitude	-5.45E-03	R^2 adj	0.849
S_{ave} *Elevation	1.32E-05	S_{ave} *Elevation	2.53E-05		
$S_{ave} * T_{norm}$	-4.30E-02	$S_{ave} * T_{norm}$	2.40E-02		
*Latitude*Longitude*	1.25E-03	*Latitude*Longitude*	2.60E-03		
Elevation T_{norm}*	-2.66E-04	*Latitude*Elevation*	-2.81E-05		
$hHMA^2$	3.36E-02	*Latitude* T_{norm}*	-7.05E-02		
S_{ave} ^{2}	-1.85E-03	*Longitude*Elevation*	-1.34E-05		
$Latitude^2$	1.86E-02	*Longitude* T_{norm}*	-2.15E-02		
$Longitude^2$	3.63E-04	*Elevation* T_{norm}*	-1.23E-04		
T_{norm}^2	1.63E+00	$Latitude^2$	-1.12E-02		
R^2 adj	0.789	$Longitude^2$	2.25E-03		
		$Elevation^2$	4.26E-08		
		Tn_{orm}^2	1.44E+00		
		R^2 adj	0.768		

AMDAT Zone = 7	
Term	**Coefficient**
(Intercept)	-4.38E+02
L	-8.27E-02
h_{PCC}	5.85E-01
h_{HMA}	2.87E-01
S_{ave}	7.76E+00
Latitude	1.24E+01
Longitude	-5.97E-02
Elevation	8.72E-04
T_{norm}	6.39E+00

$L * h_{HMA}$	1.35E-02
$h_{PCC} * h_{HMA}$	-4.28E-02
$h_{PCC} * T_{norm}$	-3.42E-01
$h_{HMA} * T_{norm}$	-1.34E-01
S_{ave} *Latitude	-2.19E-01
$S_{ave} * T_{norm}$	-4.58E-01
Latitude* T_{norm}	5.17E-01
Longitude* T_{norm}	7.36E-02
Elevation* T_{norm}	-9.08E-04
R^2 adj	0.81

Joint spacing ≥ 10 ft with joint activation through both PCC and HMA

AMDAT Zone = 1		AMDAT Zone = 2		AMDAT Zone = 3	
Term	**Coefficient**	**Term**	**Coefficient**	**Term**	**Coefficient**
(Intercept)	-4.00E+01	*(Intercept)*	1.16E+01	*(Intercept)*	-5.78E+01
L	-1.72E+00	*L*	-4.89E-01	*L*	8.40E-01
h_{PCC}	-3.82E+00	h_{PCC}	-6.23E+00	h_{PCC}	-3.07E+00
h_{HMA}	2.28E+00	h_{HMA}	2.47E+00	h_{HMA}	1.66E+00
S_{ave}	2.51E+00	S_{ave}	-2.87E-01	S_{ave}	2.90E-01
Latitude	1.58E+00	*Latitude*	-6.08E-01	*Latitude*	2.00E+00
Longitude	-1.38E+00	*Longitude*	7.87E-02	*Longitude*	-1.97E-01
Elevation	3.81E-03	*Elevation*	-2.66E-05	*Elevation*	1.22E-03
T_{norm}	2.80E+01	T_{norm}	4.12E+01	T_{norm}	3.80E+01
$L * h_{PCC}$	5.94E-01	$L * h_{PCC}$	5.92E-01	$L * h_{PCC}$	4.26E-01
$L * h_{HMA}$	-1.48E-01	$L * h_{HMA}$	-1.47E-01	$L * h_{HMA}$	-1.26E-01
$L * S_{ave}$	1.62E-02	*L*Longitude*	5.44E-03	$L * S_{ave}$	4.34E-03
*L*Elevation*	5.02E-05	*L*Elevation*	6.08E-05	*L*Elevation*	3.17E-05
$L * T_{norm}$	-1.58E+00	$L * T_{norm}$	-2.36E+00	$L * T_{norm}$	-2.52E+00
$h_{PCC} * h_{HMA}$	-1.60E-01	$h_{PCC} * h_{HMA}$	-1.50E-01	$h_{PCC} * h_{HMA}$	-9.34E-02
$h_{PCC} * T_{norm}$	-1.59E+00	h_{PCC} *S_{ave}	-1.69E-02	h_{PCC} *Latitude	2.20E-02
h_{HMA} *Longitude	-3.29E-03	h_{PCC} *Latitude	1.03E-01	$h_{PCC} * T_{norm}$	-1.89E+00
$h_{HMA} * T_{norm}$	2.57E-01	h_{PCC} *Longitude	-9.91E-03	$h_{HMA} * S_{ave}$	-1.48E-03
S_{ave} *Latitude	-2.77E-02	h_{PCC} *Elevation	1.88E-04	h_{HMA} *Tnorm	2.82E-01
S_{ave} *Longitude	3.07E-02	$h_{PCC} * T_{norm}$	-2.23E+00	S_{ave} *Latitude	-2.93E-03
S_{ave} *Elevation	2.74E-05	h_{HMA} *Latitude	-1.59E-02	S_{ave} *Longitude	1.44E-03
Latitude* T_{norm}	-1.38E-01	h_{HMA} *Elevation	-1.92E-05	$S_{ave} * T_{norm}$	-4.73E-02
*Longitude*Elevation*	-5.04E-05	$h_{HMA} * T_{norm}$	2.87E-01	*Latitude*Longitude*	7.35E-03
Elevation* T_{norm}	-6.39E-04	S_{ave} *Latitude	6.10E-03	*Latitude*Elevation*	-2.31E-05
h_{HMA}^2	2.01E-02	S_{ave} *Longitude	1.00E-03	Latitude* T_{norm}	-1.05E-01
S_{ave}^2	-3.91E-02	S_{ave} *Elevation	-1.51E-05	Longitude* T_{norm}	1.41E-02
$Longitude^2$	-1.31E-03	$S_{ave} * T_{norm}$	6.60E-02	Elevation* T_{norm}	-5.90E-04
$Elevation^2$	-3.16E-08	Latitude* T_{norm}	-2.15E-01	S_{ave}^2	-2.76E-03

R^2 adj	0.728	*Longitude* T_{norm}*	-2.15E-02	*Latitude^2*	-3.13E-02
		Elevation T_{norm}*	-9.85E-04	*Longitude^2*	-9.25E-04
		$h_{HMA}{}^2$	3.03E-02	R^2 adj	0.79
		Longitude^2	-6.13E-04		
		Elevation^2	5.95E-08		
		R^2 adj	0.774		
AMDAT Zone = 4		**AMDAT Zone = 5**		**AMDAT Zone = 6**	
Term	**Coefficient**	**Term**	**Coefficient**	**Term**	**Coefficient**
(Intercept)	-1.70E+01	*(Intercept)*	1.08E+02	*(Intercept)*	-1.25E+03
L	-1.18E+00	*L*	-1.48E+00	*L*	-3.32E-02
h_{PCC}	-1.51E+00	h_{PCC}	-1.91E+00	h_{PCC}	-5.65E-01
h_{HMA}	1.03E+00	h_{HMA}	1.13E+00	h_{HMA}	8.32E-02
S_{ave}	7.27E-01	S_{ave}	-2.29E+00	S_{ave}	2.15E+01
Latitude	-7.26E-01	*Latitude*	-2.44E+00	*Latitude*	-1.19E+00
Longitude	-9.24E-03	*Longitude*	4.67E-04	*Longitude*	1.24E+01
Elevation	-1.37E-03	*Elevation*	3.09E-03	*Elevation*	-1.00E-01
T_{norm}	3.88E+01	T_{norm}	4.09E+01	T_{norm}	7.50E+01
*L** h_{PCC}	3.15E-01	*L** h_{PCC}	2.28E-01	*L** h_{PCC}	1.56E-01
*L** h_{HMA}	-1.04E-01	*L** h_{HMA}	-8.17E-02	*L** h_{HMA}	-4.50E-02
*L*Latitude*	6.66E-02	*L*Latitude*	6.55E-02	*L*Longitude*	1.34E-02
*L*Longitude*	4.77E-03	*L*Longitude*	9.75E-03	*L** T_{norm}	-1.92E+00
*L** T_{norm}	-2.69E+00	*L** T_{norm}	-2.37E+00	h_{PCC} * T_{norm}	-1.16E+00
*HPCC** h_{HMA}	-3.80E-02	h_{PCC} * h_{HMA}	-3.78E-02	h_{HMA} * T_{norm}	4.09E-01
*HPCC** T_{norm}	-1.72E+00	h_{PCC} *Latitude	2.93E-02	S_{ave} *Longitude	-2.09E-01
h_{HMA} * T_{norm}	2.91E-01	h_{PCC} * T_{norm}	-1.34E+00	S_{ave} * T_{norm}	-1.05E+00
S_{ave} *Elevation	1.78E-05	h_{HMA} * S_{ave}	3.51E-03	*Latitude*Elevation*	3.26E-03
S_{ave} *T_{norm}	-1.21E-01	h_{HMA} *Latitude	-1.24E-02	*Latitude** T_{norm}	5.78E-01
*Longitude** T_{norm}	-2.91E-02	h_{HMA} *Elevation	-2.27E-05	*Longitude** T_{norm}	-2.02E-01
$S_{ave}{}^2$	-5.21E-03	h_{HMA} * T_{norm}	3.53E-01	*Elevation** T_{norm}	4.80E-03
Elevation^2	4.12E-08	S_{ave} *Longitude	-4.99E-03	$T_{norm}{}^2$	4.26E+00
$T_{norm}{}^2$	1.93E+00	*Latitude*Longitude*	7.89E-03	R^2 adj	0.805
R^2 adj	0.817	*Latitude*Elevation*	-8.20E-05		
		*Latitude** T_{norm}	-3.74E-01		
		*Longitude** T_{norm}	-9.14E-02		
		*Elevation** T_{norm}	-1.38E-04		
		$h_{HMA}{}^2$	-1.41E-02		
		$S_{ave}{}^2$	2.11E-02		
		Latitude^2	1.93E-02		
		$T_{norm}{}^2$	3.62E+00		
		R^2 adj	0.803		
AMDAT Zone = 7					

Term	Coefficient
(Intercept)	-7.27E+01
L	9.21E-01
h_{PCC}	1.28E-02
h_{HMA}	-2.15E-02
S_{ave}	1.48E+00
Latitude	-4.33E-01
Longitude	5.39E-01
Elevation	7.10E-04
T_{norm}	3.01E+00
$L * h_{PCC}$	-6.93E-02
*L*Latitude*	3.77E-02
*L*Longitude*	-4.97E-03
$L * T_{norm}$	-1.24E+00
h_{PCC} **Longitude*	6.90E-03
$h_{HMA} * T_{norm}$	3.27E-01
S_{ave}**Longitude*	-1.01E-02
$S_{ave} * T_{norm}$	-3.26E-01
*Longitude** T_{norm}	8.28E-02
*Elevation** T_{norm}	-7.42E-04
h_{HMA}^{2}	-2.40E-02
T_{norm}^{2}	9.33E+00
R^2 adj	0.811

All adjustment factors are presented with regard to the reference month (January for fatigue and September for faulting), thus the adjustment factor for the reference month is always one. Therefore, only the monthly HMA modulus for the reference month needs to be determined. To calculate the remaining monthly HMA modulus values, this reference value is multiplied by monthly adjustment factors from Equations (21) and (22) and Table 4. Regressions were developed for the three different design methods for all 7 AMDAT zones for a total of 21

regressions each for the fatigue and faulting models. The developed regression models are summarized below with all coefficients and R^2 values for both methods and all seven zones in Equations (23) and (24) for fatigue and faulting respectively, and Table 5.

$$E_{HMA(Ref)}^{fatigue} = C_1 + C_2 * T_{Mid-Depth(Ref)} + C_3 * h_{HMA} + C_4 * Latitude + C_5 * Longitude + C_6 * Elevation \quad (23)$$

$$E_{HMA(Ref)}^{faulting} = \sum(Terms \times Coefficients) \quad (24)$$

where,

$E_{HMA(Ref)}$ is the reference month HMA modulus, psi.

$T_{Mid-Depth(Ref)}$ is the reference month mid-depth HMA temperature, ºF.

Table 5: Reference month HMA modulus coefficients by zone for (a) fatigue analysis and (b) faulting analysis.

(a) Fatigue analysis (reference month is January)							
≤ 4.5 ft × 4.5 ft joint spacing	**C1**	**C2**	**C3**	**C4**	**C5**	**C6**	**R^2**
Zone 1	6902212	-58060.5	-36684	-48511	-3980.3	-9.91	0.901
Zone 2	5746174	-48590	-45205	-32771	505.3	-31.81	0.687
Zone 3	3919812	-20078.4	-45233	17658	-12374.7	52.25	0.654
Zone 4	3951615	-52629	-46317	25747	-2356	17.61	0.859
Zone 5	6172028	-62418	-69110	-31747	1793.9	4.801	0.908
Zone 6	5657489	-48939	-52613	-11091	-7769	-4.95	0.911
Zone 7	4050512	-39010	-56927	35689	-10707	88.486	0.856
> 4.5 ft and ≤ 7 ft joint spacing	**C1**	**C2**	**C3**	**C4**	**C5**	**C6**	**R^2**
Zone 1	516844	-35706	-65351	-22220	-6306	30.121	0.623
Zone 2	5396644	-40139	-89164	-32803	4454	-45.742	0.558
Zone 3	333077	-26639	-73246	30958	-7350	64.1	0.546
Zone 4	3458108	-35086	-31812	20508	-1956	47.1	0.590
Zone 5	3849527	-45022	-3932	2710	1245	48.4	0.723

Zone 6	3912042	-40680	-8978	-12689	3328	25.1	0.798
Zone 7	3901375	-44662	-10529	36735	-7709	15.89	0.824
> 7 ft transverse joint spacing	**C1**	**C2**	**C3**	**C4**	**C5**	**C6**	**R^2**
Zone 1	2491478	-10560	-142588	-11145	1813.8	-0.423	0.681
Zone 2	2076287	-6963	-146622	-198	596.9	4.914	0.711
Zone 3	2173722	-586.2	-145128	-4937	-381.7	3.028	0.706
Zone 4	2058023	-1519	-137632	99	-1295.7	5.391	0.685
Zone 5	2174744	-6379	-123582	-3127	69.6	-0.576	0.627
Zone 6	1718085	-2601	-107895	-3189	1959	-9.12	0.594
Zone 7	1734430	-7589	-112461	7729	1172	-2.32	0.687

(b) Faulting analysis (reference month is September)					
Joint spacing < 10 ft with joint activation through PCC only					
AMDAT Zone = 1		**AMDAT Zone = 2**		**AMDAT Zone = 3**	
Term	**Coefficient**	**Term**	**Coefficient**	**Term**	**Coefficient**
(Intercept)	6.91E+04	*(Intercept)*	1.85E+06	*(Intercept)*	7.89E+06
L	-3.93E+05	L	-4.05E+05	L	-2.42E+05
h_{PCC}	-5.73E+05	h_{PCC}	-5.51E+05	h_{PCC}	-1.10E+06
h_{HMA}	5.44E+05	h_{HMA}	5.43E+05	h_{HMA}	5.13E+05
S_{ave}	1.02E+05	S_{ave}	6.17E+04	S_{ave}	4.04E+02
Latitude	4.52E+04	*Latitude*	-8.30E+04	*Latitude*	-8.67E+04
Longitude	-1.41E+03	*Longitude*	8.02E+04	*Longitude*	-2.76E+04
Elevation	-1.11E+02	*Elevation*	-9.05E+02	*Elevation*	-3.78E+02
$T_{Mid\text{-}Depth(Ref)}$	-1.25E+04	$T_{Mid\text{-}Depth(Ref)}$	-2.94E+04	$T_{Mid\text{-}Depth(Ref)}$	-4.94E+03
$L * h_{PCC}$	7.08E+04	$L * h_{PCC}$	7.39E+04	$L * h_{PCC}$	8.01E+04
$h_{PCC} * S_{ave}$	-3.17E+03	h_{HMA} *Latitude	-7.39E+03	$L * T_{Mid\text{-}Depth(Ref)}$	-2.42E+03
$h_{PCC} * T_{Mid\text{-}Depth(Ref)}$	3.28E+03	h_{HMA} *Longitude	7.10E+02	$h_{PCC} * T_{Mid\text{-}Depth(Ref)}$	6.10E+03
h_{HMA} *Latitude	-2.67E+03	h_{HMA} *Elevation	-1.36E+01	$h_{HMA} * S_{ave}$	-8.08E+02
$h_{HMA} * T_{Mid\text{-}Depth(Ref)}$	-2.83E+03	S_{ave} *Longitude	-1.63E+03	$h_{HMA} * T_{Mid\text{-}Depth(Ref)}$	-1.88E+03
S_{ave} *Latitude	-1.09E+03	$S_{ave} * T_{Mid\text{-}Depth(Ref)}$	-2.25E+03	$S_{ave} * T_{Mid\text{-}Depth(Ref)}$	-5.20E+02
*Longitude*Elevation*	2.50E+00	*Latitude*Longitude*	-9.92E+02	*Latitude*Longitude*	7.17E+02
*Elevation** $T_{Mid\text{-}Depth(Ref)}$	-2.35E+00	*Latitude** $T_{Mid\text{-}Depth(Ref)}$	2.45E+03	*Longitude*Elevation*	-2.99E+00
h_{HMA}^2	-1.60E+04	*Elevation** $T_{Mid\text{-}Depth(Ref)}$	1.31E+01	*Elevation** $T_{Mid\text{-}Depth(Ref)}$	7.67E+00

S_{ave}^2	-3.38E+02	h_{HMA}^2	-1.96E+04	h_{HMA}^2	-2.34E+04
R^2 adj	0.791	S_{ave}^2	2.39E+03	S_{ave}^2	4.39E+02
		Longitude^2	2.83E+02	R^2 adj	0.727
		Elevation^2	-1.92E-02		
		R^2 adj	0.765		
AMDAT Zone = 4		**AMDAT Zone = 5**		**AMDAT Zone = 6**	
Term	**Coefficient**	**Term**	**Coefficient**	**Term**	**Coefficient**
(Intercept)	-2.06E+07	*(Intercept)*	2.00E+06	*(Intercept)*	4.05E+06
L	-2.33E+05	*L*	-3.41E+05	*L*	-2.67E+05
h_{PCC}	-1.15E+06	h_{PCC}	-4.44E+05	h_{PCC}	-3.50E+05
h_{HMA}	5.15E+05	h_{HMA}	3.08E+05	h_{HMA}	2.83E+05
S_{ave}	8.11E+04	S_{ave}	1.13E+05	*Longitude*	-3.06E+03
Latitude	1.23E+06	*Latitude*	-2.96E+05	*Elevation*	2.35E+01
Elevation	3.25E+02	*Longitude*	6.95E+04	$T_{Mid\text{-}Depth(Ref)}$	-1.73E+04
$T_{Mid\text{-}Depth(Ref)}$	-1.48E+04	*Elevation*	2.76E+01	$L^* h_{PCC}$	4.81E+04
$L^* h_{PCC}$	8.58E+04	$T_{Mid\text{-}Depth(Ref)}$	-1.42E+04	$h_{HMA} * T_{Mid\text{-}Depth(Ref)}$	-1.64E+03
$L^* T_{Mid\text{-}Depth(Ref)}$	-2.83E+03	$L^* h_{PCC}$	6.13E+04	h_{HMA}^2	-9.96E+03
$h_{PCC} * T_{Mid\text{-}Depth(Ref)}$	6.16E+03	*HHMA** $T_{Mid\text{-}Depth(Ref)}$	-1.56E+03	R^2 adj	0.886
$h_{HMA} * T_{Mid\text{-}Depth(Ref)}$	-2.75E+03	S_{ave} *Longitude*	-1.15E+03		
S_{ave} *Latitude*	-2.20E+03	h_{HMA}^2	-1.25E+04		
S_{ave} *Elevation*	-4.79E+00	$Latitude^2$	4.42E+03		
h_{HMA}^2	-2.10E+04	R^2 adj	0.779		
$Latitude^2$	-1.48E+04				
R^2 adj	0.743				
AMDAT Zone = 7					
Term	**Coefficient**				
(Intercept)	1.17E+07				
L	2.83E+04				
h_{PCC}	-1.13E+04				
h_{HMA}	9.47E+04				
S_{ave}	-5.52E+04				
Latitude	-2.82E+05				
Longitude	-9.41E+04				
$T_{Mid\text{-}Depth(Ref)}$	-2.69E+03				
$L^* S_{ave}$	8.30E+02				
$L^* T_{Mid\text{-}Depth(Ref)}$	-7.92E+02				
h_{HMA} *Longitude*	3.28E+02				
$h_{HMA} * T_{Mid\text{-}Depth(Ref)}$	-7.29E+02				

*Latitude*Longitude*	3.43E+03
h_{HMA}^{2}	-4.44E+03
R^2 adj	0.965

Joint spacing < 10 ft with joint activation through both PCC and HMA

AMDAT Zone = 1		AMDAT Zone = 2		AMDAT Zone = 3	
Term	**Coefficient**	**Term**	**Coefficient**	**Term**	**Coefficient**
(Intercept)	6.92E+04	*(Intercept)*	1.85E+06	*(Intercept)*	7.89E+06
L	-3.93E+05	*L*	-4.05E+05	*L*	-2.42E+05
h_{PCC}	-5.73E+05	h_{PCC}	-5.51E+05	h_{PCC}	-1.10E+06
h_{HMA}	5.44E+05	h_{HMA}	5.43E+05	h_{HMA}	5.13E+05
S_{ave}	1.02E+05	S_{ave}	6.17E+04	S_{ave}	4.04E+02
Latitude	4.52E+04	*Latitude*	-8.30E+04	*Latitude*	-8.67E+04
Longitude	-1.41E+03	*Longitude*	8.02E+04	*Longitude*	-2.76E+04
Elevation	-1.11E+02	*Elevation*	-9.05E+02	*Elevation*	-3.78E+02
$T_{Mid\text{-}Depth(Ref)}$	-1.25E+04	$T_{Mid\text{-}Depth(Ref)}$	-2.94E+04	$T_{Mid\text{-}Depth(Ref)}$	-4.94E+03
$L^* h_{PCC}$	7.08E+04	$L^* h_{PCC}$	7.39E+04	$L^* h_{PCC}$	8.01E+04
$h_{PCC} * S_{ave}$	-3.17E+03	h_{HMA} *Latitude	-7.39E+03	$L^* T_{Mid\text{-}Depth(Ref)}$	-2.42E+03
$h_{PCC} * T_{Mid\text{-}Depth(Ref)}$	3.28E+03	h_{HMA} *Longitude	7.10E+02	$h_{PCC} * T_{Mid\text{-}Depth(Ref)}$	6.10E+03
h_{HMA} *Latitude	-2.67E+03	h_{HMA} *Elevation	-1.36E+01	$h_{HMA} * S_{ave}$	-8.08E+02
$h_{HMA} * T_{Mid\text{-}Depth(Ref)}$	-2.83E+03	S_{ave} *Longitude	-1.63E+03	$h_{HMA} * T_{Mid\text{-}Depth(Ref)}$	-1.88E+03
S_{ave} *Latitude	-1.09E+03	$S_{ave} * T_{Mid\text{-}Depth(Ref)}$	-2.25E+03	$S_{ave} * T_{Mid\text{-}Depth(Ref)}$	-5.20E+02
*Longitude*Elevation*	2.50E+00	*Latitude*Longitude*	-9.92E+02	*Latitude*Longitude*	7.17E+02
*Elevation** $T_{Mid\text{-}Depth(Ref)}$	-2.35E+00	*Latitude** $T_{Mid\text{-}Depth(Ref)}$	2.45E+03	*Longitude*Elevation*	-2.99E+00
h_{HMA}^{2}	-1.60E+04	*Elevation** $T_{Mid\text{-}Depth(Ref)}$	1.31E+01	*Elevation** $T_{Mid\text{-}Depth(Ref)}$	7.67E+00
S_{ave}^{2}	-3.38E+02	h_{HMA}^{2}	-1.96E+04	h_{HMA}^{2}	-2.34E+04
R^2 adj	0.791	S_{ave}^{2}	2.39E+03	S_{ave}^{2}	4.39E+02
		$Longitude^2$	2.83E+02	R^2 adj	0.727
		$Elevation^2$	-1.92E-02		
		R^2 adj	0.765		

AMDAT Zone = 4		AMDAT Zone = 5		AMDAT Zone = 6	
Term	**Coefficient**	**Term**	**Coefficient**	**Term**	**Coefficient**
(Intercept)	-2.06E+07	*(Intercept)*	2.00E+06	*(Intercept)*	4.05E+06
L	-2.33E+05	*L*	-3.41E+05	*L*	-2.67E+05
h_{PCC}	-1.15E+06	h_{PCC}	-4.44E+05	h_{PCC}	-3.50E+05
h_{HMA}	5.15E+05	h_{HMA}	3.08E+05	h_{HMA}	2.83E+05
S_{ave}	8.11E+04	S_{ave}	1.13E+05	*Longitude*	-3.06E+03
Latitude	1.23E+06	*Latitude*	-2.96E+05	*Elevation*	2.35E+01
Elevation	3.25E+02	*Longitude*	6.95E+04	$T_{Mid\text{-}Depth(Ref)}$	-1.73E+04
$T_{Mid\text{-}Depth(Ref)}$	-1.48E+04	*Elevation*	2.76E+01	$L^* h_{PCC}$	4.81E+04
$L^* h_{PCC}$	8.58E+04	$T_{Mid\text{-}Depth(Ref)}$	-1.42E+04	$h_{HMA} * T_{Mid\text{-}Depth(Ref)}$	-1.64E+03
$L^* T_{Mid\text{-}Depth(Ref)}$	-2.83E+03	$L^* h_{PCC}$	6.13E+04	h_{HMA}^{2}	-9.96E+03

$h_{PCC} * T_{Mid\text{-}Depth(Ref)}$	6.16E+03	$h_{HMA} * T_{Mid\text{-}Depth(Ref)}$	-1.56E+03	R^2 adj	0.886
$h_{HMA} * T_{Mid\text{-}Depth(Ref)}$	-2.75E+03	S_{ave} *Longitude	-1.15E+03		
S_{ave} *Latitude	-2.20E+03	h_{HMA}^2	-1.25E+04		
S_{ave} *Elevation	-4.79E+00	$Latitude^2$	4.42E+03		
h_{HMA}^2	-2.10E+04	R^2 adj	0.779		
$Latitude^2$	-1.48E+04				
R^2 adj	0.743				
AMDAT Zone = 7					
Term	**Coefficient**				
(Intercept)	1.17E+07				
L	2.83E+04				
h_{PCC}	-1.13E+04				
h_{HMA}	9.47E+04				
S_{ave}	-5.52E+04				
Latitude	-2.82E+05				
Longitude	-9.41E+04				
$T_{Mid\text{-}Depth(Ref)}$	-2.69E+03				
$L* S_{ave}$	8.30E+02				
$L* T_{Mid\text{-}Depth(Ref)}$	-7.92E+02				
h_{HMA} *Longitude	3.28E+02				
$h_{HMA} * T_{Mid\text{-}Depth(Ref)}$	-7.29E+02				
*Latitude*Longitude*	3.43E+03				
h_{HMA}^2	-4.44E+03				
R^2 adj	0.965				

Joint spacing ≥ 10 ft with joint activation through both PCC and HMA

AMDAT Zone = 1		**AMDAT Zone = 2**		**AMDAT Zone = 3**	
Term	**Coefficient**	**Term**	**Coefficient**	**Term**	**Coefficient**
(Intercept)	2.08E+07	(Intercept)	1.49E+07	(Intercept)	4.37E+07
L	-1.02E+05	*L*	-6.61E+05	*L*	-9.29E+05
h_{PCC}	7.32E+05	h_{PCC}	5.75E+05	h_{PCC}	2.96E+05
h_{HMA}	-8.96E+04	h_{HMA}	-9.61E+04	h_{HMA}	-1.34E+05
S_{ave}	-3.79E+04	S_{ave}	-1.82E+04	S_{ave}	-2.17E+05
Latitude	-2.81E+05	*Latitude*	-1.30E+05	*Latitude*	-1.53E+06
Elevation	-2.58E+01	*Longitude*	7.12E+04	*Longitude*	2.21E+05
$T_{Mid\text{-}Depth(Ref)}$	-3.16E+05	*Elevation*	-3.32E+02	*Elevation*	-1.25E+03
$L* h_{PCC}$	-7.52E+04	$T_{Mid\text{-}Depth(Ref)}$	-2.34E+05	$T_{Mid\text{-}Depth(Ref)}$	-2.10E+05
$L * h_{HMA}$	1.76E+04	$L * h_{PCC}$	-7.52E+04	$L * h_{PCC}$	-6.14E+04
$L * S_{ave}$	-7.17E+03	$L * h_{HMA}$	1.85E+04	$L * h_{HMA}$	1.91E+04
*L *Latitude*	4.69E+03	*L *Latitude*	2.56E+04	$L * S_{ave}$	3.53E+03

$L * T_{Mid\text{-}Depth(Ref)}$	6.55E+03	$L * Longitude$	-4.16E+03	$L * Latitude$	1.86E+04
$S_{ave} * T_{Mid\text{-}Depth(Ref)}$	1.59E+03	$L * Elevation$	3.49E+01	$L * Longitude$	-2.59E+03
$Latitude * T_{Mid\text{-}Depth(Ref)}$	2.84E+03	$h_{PCC} * Longitude$	1.61E+03	$L * Elevation$	1.13E+01
h_{HMA}^{2}	-7.86E+03	$S_{ave} * Longitude$	-1.27E+03	$L * T_{Mid\text{-}Depth(Ref)}$	2.61E+03
R^2 adj	0.871	$S_{ave} * Elevation$	-1.94E+00	$h_{PCC} * T_{Mid\text{-}Depth(Ref)}$	3.61E+03
		$S_{ave} * T_{Mid\text{-}Depth(Ref)}$	-9.06E+02	$S_{ave} * Latitude$	1.59E+03
		$Latitude * Longitude$	-6.14E+02	$S_{ave} * Longitude$	-4.12E+02
		$Longitude\ T_{Mid\text{-}Depth(Ref)}$	4.60E+02	$S_{ave} * T_{Mid\text{-}Depth(Ref)}$	1.12E+03
		h_{HMA}^{2}	-8.32E+03	$Latitude * Longitude$	-2.30E+03
		S_{ave}^{2}	1.89E+03	$Latitude * Elevation$	8.79E+00
		$Latitude^2$	-1.31E+03	$Latitude * T_{Mid\text{-}Depth(Ref)}$	3.95E+03
		$Longitude^2$	1.62E+02	$Longitude * T_{Mid\text{-}Depth(Ref)}$	-1.03E+03
		$T_{Mid\text{-}Depth(Ref)}^{2}$	1.40E+03	$Elevation * T_{Mid\text{-}Depth(Ref)}$	8.78E+00
		R^2 adj	0.904	h_{HMA}^{2}	-5.73E+03
				S_{ave}^{2}	6.07E+02
				$Latitude^2$	1.39E+04
				R^2 adj	0.914

AMDAT Zone = 4		**AMDAT Zone = 5**		**AMDAT Zone = 6**	
Term	**Coefficient**	**Term**	**Coefficient**	**Term**	**Coefficient**
(Intercept)	-4.20E+06	*(Intercept)*	5.13E+07	*(Intercept)*	1.15E+07
L	8.31E+05	L	-2.67E+05	L	1.70E+05
h_{PCC}	4.45E+05	h_{PCC}	3.86E+05	h_{PCC}	5.38E+05
h_{HMA}	-1.87E+05	h_{HMA}	-9.46E+04	h_{HMA}	-2.13E+04
S_{ave}	-8.22E+04	S_{ave}	-4.90E+05	$Latitude$	-1.21E+05
$Latitude$	6.38E+05	$Latitude$	-9.35E+05	$Longitude$	-3.61E+03
$Longitude$	9.02E+03	$Longitude$	1.63E+05	$Elevation$	-7.56E+03
$Elevation$	5.57E+02	$Elevation$	9.45E+02	$T_{Mid\text{-}Depth(Ref)}$	-9.52E+04
$T_{Mid\text{-}Depth(Ref)}$	-1.83E+05	$T_{Mid\text{-}Depth(Ref)}$	-5.35E+05	$L * h_{PCC}$	-5.61E+04
$L * h_{PCC}$	-6.33E+04	$L * h_{PCC}$	-5.55E+04	$L * h_{HMA}$	1.13E+04
$L * h_{HMA}$	1.78E+04	$L * h_{HMA}$	1.47E+04	$Elevation * T_{Mid\text{-}Depth(Ref)}$	8.20E+01
$L * S_{ave}$	9.11E+03	$L * Latitude$	-1.33E+04	h_{HMA}^{2}	-7.92E+03
$L * Latitude$	-1.97E+04	$L * Elevation$	-2.04E+01	R^2 adj	0.897
$L * Longitude$	-2.21E+03	$L * T_{Mid\text{-}Depth(Ref)}$	9.06E+03		
$L * T_{Mid\text{-}Depth(Ref)}$	-4.99E+03	$h_{PCC} * Longitude$	1.55E+03		
$h_{PCC} * Longitude$	1.73E+03	$S_{ave} * Longitude$	-6.35E+03		
$S_{ave} * Elevation$	-1.18E+01	$S_{ave} * T_{Mid\text{-}Depth(Ref)}$	-1.97E+03		

Longitude Elevation*	2.51E+00	*Latitude* Elevation*	-3.93E+01		
Latitude^2	-5.82E+03	*Latitude** $T_{Mid\text{-}Depth(Ref)}$	1.23E+04		
$T_{Mid\text{-}Depth(Ref)}$	1.24E+03	*Longitude** $T_{Mid\text{-}Depth(Ref)}$	1.16E+03		
R^2 adj	0.939	*Elevation ** $T_{Mid\text{-}Depth(Ref)}$	5.75E+00		
		$h_{HMA}{}^2$	-4.77E+03		
		$S_{ave}{}^2$	1.01E+04		
		Longitude^2	5.77E+02		
		R^2 adj	0.927		
AMDAT Zone = 7					
Term	**Coefficient**				
(Intercept)	3.20E+07				
L	-5.00E+04				
h_{PCC}	2.27E+05				
h_{HMA}	-8.81E+04				
S_{ave}	-1.22E+05				
Latitude	-1.64E+06				
Longitude	1.58E+04				
Elevation	1.11E+02				
$T_{Mid\text{-}Depth(Ref)}$	-6.04E+04				
*L *Latitude*	-1.37E+04				
*L * Elevation*	-1.30E+01				
*L** $T_{Mid\text{-}Depth(Ref)}$	4.22E+03				
h_{PCC} **Longitude*	-2.33E+03				
h_{HMA} *** $T_{Mid\text{-}Depth(Ref)}$	8.77E+02				
Latitude^2	3.38E+04				
R^2 adj	0.899				

3.3 Determination of Inputs for HMA Modulus Adjustment Factors and Reference Month HMA Modulus

The calculation of HMA modulus adjustment factors requires HMA thickness and the normalized mid-depth HMA temperature, which is dependent on the temperature region of the project location, as determined from Figure 4. The reference month HMA Modulus equation requires the HMA thickness and the latitude, longitude, and elevation of the project, which are all user inputs. Finally,

the reference month mid-depth HMA temperature is contingent on the AMDAT zone, as determined from Figure 4.

3.4 Determination of HMA Modulus

The undamaged HMA dynamic modulus is first estimated for a reference temperature of 70°F using a master curve (ARA, 2004). This undamaged HMA modulus value is then converted to a damaged HMA modulus to reflect the HMA layer condition.

MEPDG (ARA, 2004) provides the following relationship for the damaged HMA modulus:

$$E^*_{HMA(dam)} = 10^{\delta} + \frac{E^*_{HMA(dam)} - 10^{\delta}}{1 + e^{-0.3+5\times\log(\mathrm{d_{AC}})}} \quad (25)$$

where,

$E^*_{HMA(dam)}$ is the damaged HMA modulus, psi.

δ is a regression parameter and is estimated as 2.84 for the default HMA mixture used in the MEPDG.

E^*_{HMA} is the modulus for the undamaged (new) HMA mixture for a specific reduced time which in this procedure is 0.1 s.

d_{AC} is the fatigue damage in the HMA layer.

Using the above relationship and Equations (23) and (24), the reduction of HMA modulus can be determined. Figure 6 shows the relationship between HMA fatigue damage factor (d_{AC}) and the corresponding reduction factor for the HMA modulus (ΔE^*) using the fatigue cracking model.

$$\Delta E^* = \frac{E^*_{HMA} - E^*_{HMA(dam)}}{E^*_{HMA}} \quad (26)$$

where,

ΔE^* is the reduction factor for the HMA modulus.

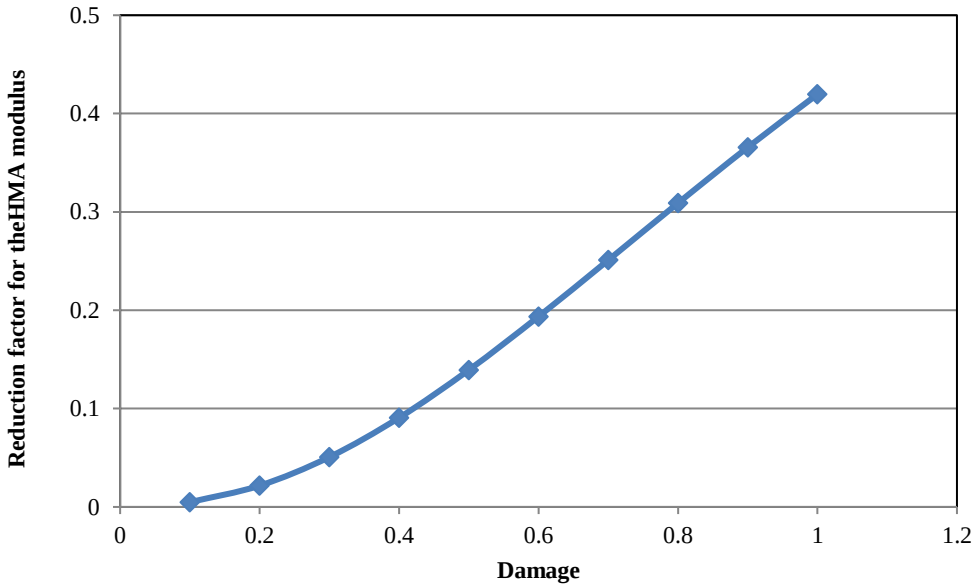

Figure 6: Relationship between the damage in the HMA layer and the corresponding reduction in the HMA modulus.

Next, the HMA damage factor is related to the HMA layer condition. According to the MEPDG (ARA, 2004), the damage factor can be related to the percentage of fatigue cracking as seen in Figure 7. For the application of bonded concrete overlays, Harrington (2008) recommends that fatigue cracking be less than 15% for primary and secondary roadways. In this procedure, the HMA base for the whitetopping is categorized into 'adequate' or 'marginal' based on the current condition. 'Adequate' HMA conditions represent approximately 0-8% fatigue cracking and a damage factor of 0.3; and 'marginal' HMA conditions represent approximately 8-20% fatigue cracking and a damage factor of 0.4. This is converted to HMA layer condition reduction percentages of 5 and 12.5 percent, respectively, as presented in Table 6.

Table 6: Reduction factor for the HMA modulus.

Existing HMA pavement	Fatigue cracking, %	Damage factor	HMA modulus reduction, %
Adequate	0-8	0.3	5
Marginal	8-20	0.4	12.5

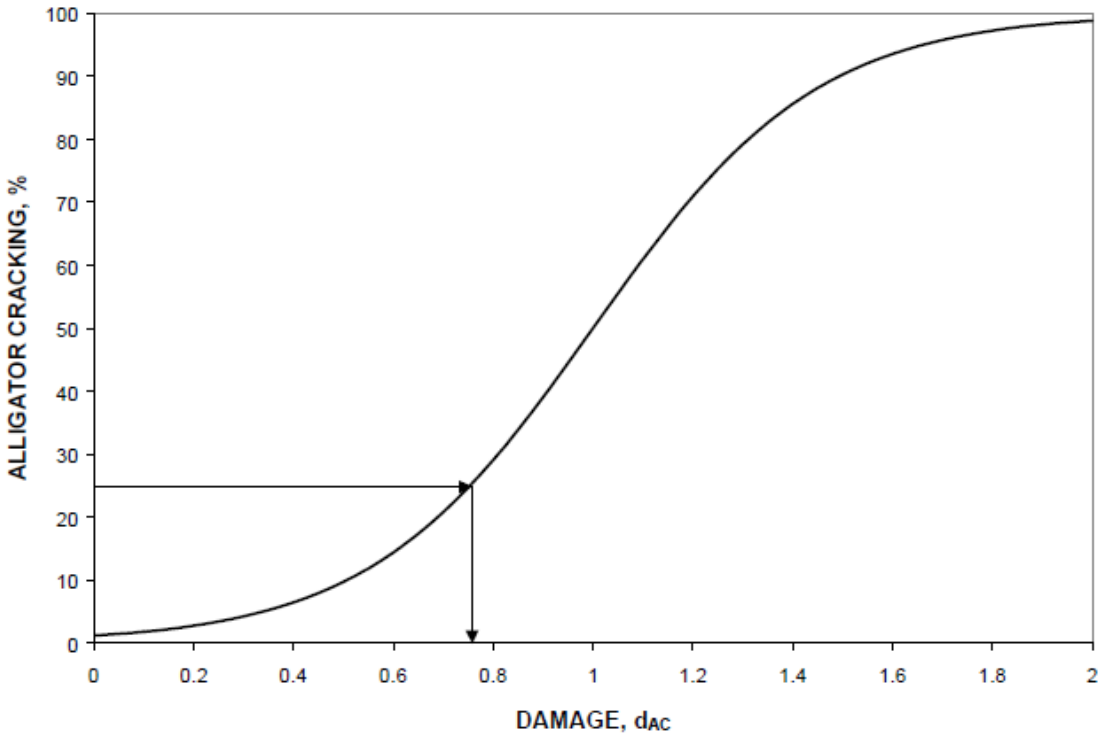

Figure 7: Relationship between alligator/fatigue cracking and damage factor (ARA, 2004).

4. Structural and Fatigue Analysis

The available design procedures specified for whitetopping are developed under the assumption that the failure modes of whitetopping are a function of the PCC thickness; specifically, ultra-thin whitetopping (UTW) failure is governed by corner cracking and thin whitetopping (TWT) failure is governed by transverse cracking. However, a performance review indicates that the actual failure modes are dictated more by slab size than PCC overlay thickness. Whitetopping projects with a 6 ft × 6 ft joint spacing more frequently experience longitudinal cracking while smaller slabs (such as 3ft × 3ft and 4ft × 4ft) experience corner cracking. This trend can be observed through the distress pattern observed in Minnesota Road Research Facility (MnROAD) whitetopping projects, as shown in Figure 8. A review of the performance of whitetopping sections across the United States supports these conclusions (Li et al 2013). Therefore, different sets of structural equations are used in this design procedure that are for the full lane width, mid-size slabs (greater than 4.5 ft and less than or equal to 7 ft joint square slabs) and smaller slabs (joint spacing

less than or equal to 4.5 ft × 4.5 ft), respectively. It is assumed that good jointing practices will be applied and the length to width ratio of the slab will be kept between 1:1 to 1:1.25.

Based on economic considerations, the design thickness in this procedure is limited to 5.5 in for smaller slabs and 6.5 in for larger slabs. For functionality considerations, the recommended minimum PCC thickness is 3.0 in and the minimum HMA layer thickness is also 3.0 in. Additionally, the existing HMA layer thickness is limited to 7 in for the structural and fatigue equations. The benefits of thicker HMA thicknesses diminishes as the HMA thickness becomes increasingly larger than 7 in. The temperature gradient calculations, however, use the given HMA layer thickness and are not limited but provide a limit for the HMA layer stiffness value using similar logic.

(a) Cell 60: 5in; 6ft × 5ft (March 2009)

(b) Cell 63: 4in; 6ft × 5ft (March 2009)

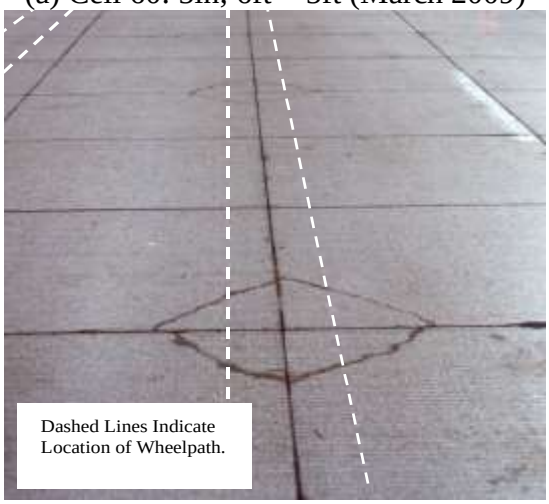

(c) Cell 94: 3in; 4ft × 4ft (2001)

(d) Cell 94: 3in; 4ft × 4ft (2003)

(e) S.H. 119 Test Section No. 2;

Figure 8: Corner, longitudinal and cracking in different slab sizes (Vandenbossche, 2001; Burnham, 2005 and CDOT 2004).

4.1 Design Stress for Slabs Joint Spacing > 4.5 ft and ≤ 7 ft

The predominant failure mode of whitetopping with a 6-ft longitudinal joint spacing was recently identified to be longitudinal cracking in the wheelpath (Li et al 2013). As no structural model was available for this type of distress in existing design procedures, a new structural model was developed to better predict the critical stresses and therefore to provide a more accurate design. A specific 3-D FE model was developed in this study, which was validated by matching the deflections with the FWD data. A database was generated for regression analysis by using a parameter matrix covering the typical ranges of whitetopping structural features.

4.1.1. Mechanical Load-Induced Stress

The critical tensile stress (σ_{18}) in a slab due to an 18-kip ESAL load is given by:

$$\sigma_{Wheel} = \frac{e^{\frac{\left(9.13668-0.0512h_{HMA}^2+8.6096h_{PCC}\right)-\log(NA)\left[27.4911-7.7478h_{PCC}+7.7478\log(E_{HMA})\right]}{15}}}{1.14}+10 \quad (27)$$

where,

σ_{Wheel} = maximum stress in the PCC overlay under 18-kip wheel load, psi.

h_{HMA} = thickness of the HMA layer, in.

h_{PCC}= thickness of PCC overlay, in.

E_{HMA} = HMA modulus of elasticity, psi.

k = modulus of subgrade reaction, psi/in.

NA = neutral axis from top of PCC overlay, in, which is given in Equation (28).

$$NA = \frac{(E_{PCC}h_{PCC}^2)/2 + \left(E_{HMA}h_{HMA}\right)\left(h_{PCC} + h_{HMA}/2\right)}{E_{PCC}h_{PCC} + E_{HMA}h_{HMA}} \quad (28)$$

where,

E_{PCC} is the PCC elastic modulus, psi and can be estimated from the standard ACI correlation given by:

$$E_{PCC} = 57{,}000\sqrt{f_c'} \quad (29)$$

where,

f'_c is the 28-day compressive strength of the concrete, psi.

4.1.2. Temperature-Induced Stress

The critical temperature-induced stress (σ_T) developed from field measurements by the Colorado Department of Transportation (CDOT) was issued for designing whitetopping projects with a joint spacing greater than 4 ft ×4 ft. Details for the CDOT method of designing whitetopping projects can be found in the work of Sheehan et al. (2004).

The critical temperature-induced stress (σ_T) is described as a percent change in stress from a zero gradient condition and can be calculated as:

$$\sigma_T = CTE^{1.07} \times \Delta T \times (0.0278 \times \Delta T + 0.3334) h_{PCC}^{[0.195812 \log(h_{HMA}) + 1.45028]} \quad (30)$$

where,

CTE is the coefficient of thermal expansion, 10^{-6} in/in/°F.

ΔT is the effective equivalent linear temperature gradient (EELTG), °F/in.

4.1.3. Design Stress

The design stress (σ_{Design}) is the sum of the adjusted load- and temperature-induced stresses given by:

$$\sigma_{design} = \sigma_{18} \times F_{stress} + \sigma_T \quad (31)$$

where,

F_{stress} is the stress adjustment factor. The details for the calculation of F_{stress} are presented in Section 4.7.

The performance prediction showed that the model was sensitive to the HMA thickness, especially for extreme values, such as less than 3 in or greater than 8 in. To compensate for this sensitivity, an effective HMA thickness (h^*_{HMA}) is employed in the calculation, as presented in Equation (32). h^*_{HMA} is used in both the structural model and the stress adjustment factor.

$$h^*_{HMA} = (5 \cdot h_{HMA} + 9)/7 \quad (32)$$

4.2. Design Stress for Slabs with Joint Spacing Less than or Equal to 4.5ft × 4.5ft

For joint spacing less than or equal to 4ft × 4ft, the structural equations developed by the by Wu et al. in 1998 to address corner cracks are adopted.

4.2.1. Mechanical Load-Induced Stress

The critical tensile stress (σ_{18}) in a slab due to an 18-kip ESAL load is given by:

$$\log(\sigma_{18}) = 5.025 - 0.465\log(k) + 0.686\log\left({L}/{l_e}\right) - 1.291\log(l_e) \quad (33)$$

where,

k is the modulus of subgrade reaction, psi/in.

L is the slab length (assuming square slabs), in.

l_e is the effective radius of relative stiffness, in.

h_{HMA} is the HMA thickness after milling, in.

h_{PCC} is the PCC overlay thickness, in.

E_{HMA} is the HMA modulus, psi.

The effective radius of relative stiffness (l_e) for a fully bonded composite pavement is computed using the moment of inertia and the modulus of subgrade reaction as described by:

$$l_e = \left[\frac{(I_m)}{(1-0.15^2)\times k}\right]^{0.25} \quad (34)$$

The moment of inertia (I_m) calculation is described by:

$$I_m = \frac{(E_{PCC}h_{PCC}^3)}{12} + E_{PCC}h_{PCC}\left(NA - \frac{(h_{PCC})}{2}\right)^2 + \frac{(E_{HMA}h_{HMA}^3)}{12} + E_{HMA}h_{HMA}\left(h_{PCC} - NA + \frac{(h_{HMA})}{2}\right)^2 \quad (35)$$

where,

The neutral axis (NA) of the composite pavement measured from the top of the concrete layer is described by Equation (28).

4.2.2. Temperature-Induced Stress

The temperature-induced stress (σ_T) is described by:

$$\sigma_T = 28.037 - 3.496(CTE \times \Delta T) - 18.382\left(\frac{L}{l_e}\right) \quad (36)$$

where,

CTE is the coefficient of thermal expansion, 10^{-6} in/in/°F.

4.2.3. Design Stress

The design stress (σ_{Design}) is the sum of the load- and temperature-induced stresses, as shown in Equation (31).

4.3 Design Stress for Slabs Full Lane Width

The performance data from MnROAD and CDOT indicated that the longitudinal cracking at mid-panel occurred shortly after the 12-ft PCC overlay was constructed but was not followed by additional longitudinal cracking. Unlike the longitudinal cracking in 6-ft slabs, longitudinal cracking in 12-ft slabs are typically located at the mid-slab and not in the wheelpath. The riding quality of the pavement is rarely affected by the mid-slab longitudinal crack and continued deterioration tends not to occur since they are not in the wheelpath. Therefore, the primary mode of failure considered in this design for these slab sizes is transverse cracking.

The structural equations developed for the Colorado Department of Transportation (CDOT) by Sheehan et al. (2004) are adopted here to account for the development of transverse cracking in the larger slab sizes that are a full lane width wide.

4.3.1. Mechanical Load-Induced Stress

The critical tensile stress (σ_{18}) in a slab due to an 18-kip ESAL load is given by:

$$\sigma_{18} = \left[18.879 + 2.918\,{h_{PCC}}/{h_{HMA}} + 425.44/l_e - 6.955 \times 10^{-6} E_{HMA} - 9.0366\log(k) + 0.0133L\right]^2 \times \frac{18}{20} \quad (37)$$

where,

σ_{18} = maximum stress in the PCC overlay under 18-kip wheel load, psi.

NA = neutral axis from top of PCC overlay, in, which is given in Equation (28).

k is the modulus of subgrade reaction, psi/in.

L is the slab length (assuming square slabs), in.

h_{HMA} is the HMA thickness after milling, in.

h_{PCC} is the PCC overlay thickness, in.

E_{HMA} is the HMA modulus, psi.

l_e is the effective radius of relative stiffness, in.

The effective radius of relative stiffness (l_e) for a fully bonded composite pavement is described by:

$$l_e = \left\{ \frac{E_{PCC} \times \left[\frac{h_{PCC}^3}{12} + h_{PCC} \times \left(NA - \frac{h_{PCC}}{2} \right)^2 \right]}{(1 - \mu_{PCC}^2) \times k} + \frac{E_{HMA} \times \left[\frac{h_{HMA}^3}{12} + h_{HMA} \times \left(h_{PCC} - NA + \frac{h_{HMA}}{2} \right)^2 \right]}{(1 - \mu_{HMA}^2) \times k} \right\}^{0.25} \quad (38)$$

where,

μ_{PCC}^2 is the Poisson's ratio for the PCC.

4.3.2. Temperature-Induced Stress

The critical temperature-induced stress (σ_T) at the same critical location as the load-induced stress is described as a percent change in stress from zero gradient that can be calculated as:

$$\sigma_T = (3.85 \times \Delta T)\% \times \sigma_{18} \quad (39)$$

where,

ΔT is the effective equivalent linear temperature gradient (EELTG), °F/in.

4.3.3. Design Stress

The design stress (σ_{Design}) is the sum of the load- and temperature-induced stresses, as shown in Equation (40).

The design stress (σ_{Design}) is the sum of the adjusted load- and temperature-induced stresses given by:

$$\sigma_{design} = \sigma_{18} \times F_{stress} + \sigma_T \quad (40)$$

where,

F_{stress} is the stress adjustment factor. As there is no performance data available, the stress adjustment factor, 1.51, developed by CDOT is used.

4.4 Allowable Fatigue Using the PCC Fatigue Equation

The fatigue equation developed by Riley et al. (2005) is used to determine the amount of allowable load repetitions, N_f, as described by:

$$\log(N_f) = \left[\frac{-SR^{-10.24}\log(R)}{0.0112}\right]^{0.217} \quad (41)$$

where,

SR is the stress ratio as defined in Equation (34).

R is the effective reliability taken as 85% in this procedure (other values could be used, but 85% is recommended).

$$SR = \frac{\sigma_{Design}}{\left(1 + R_{150}^{150}\right) \times M_R} \quad (42)$$

where,

R_{150}^{150} is the residual strength ratio characterizing the contribution of the fiber-reinforcement in concrete mixes. The details for the calculation of $R_{150}^{150}$are presented in Section 4.5.

M_R is the modulus of rupture of the PCC overlay, psi and is estimated from the ACI relationship given by:

$$M_R = 2.30 f_c{}'^{2/3} \quad (43)$$

where,

f_c' is the compressive strength of the PCC, psi.

4.5 Fiber Consideration

The use of structural fibers can be considered for whitetopping projects, particularly for PCC overlay thicknesses less than or equal to 4 in. The methodology for accounting for the contribution of fiber, developed by the Illinois Center for Transportation (Roesler et al, 2008), is adopted in this design. The performance of the whitetopping is enhanced with the inclusion of fiber because of an increased residual strength ratio of the fiber reinforced concrete (FRC). It is hypothesized that the enhanced performance of the FRC whitetopping can be accounted for by adding the residual strength to the modulus of rupture. Therefore, the equivalent stress ratio for the FRC whitetopping can be expressed as Equation (42) with residual strength added to M_R.

The user can provide the quantity of fiber in terms of weight in pounds per cubic yard of concrete. This information is then used to determine the volumetric quantity of fiber in the mix, which is then used in subsequent calculations.

The absolute volume of fiber is given by:

$$V_{Fiber}^{input} = \frac{W_{Fiber}}{SG \times 62.4 \times 27} \tag{44}$$

where,

V_{Fiber}^{input} is the volume content of the fiber, %.

W_{Fiber} is the weight of the fiber, lb/yd^3.

SG is the specific gravity of the fiber.

The stress factor used throughout this section is the ratio of the enhanced modulus of rupture (considering residual strength) to the original modulus of rupture of the concrete. These stress factors are established based on experimental results. The interpolated stress factors (*ISF*) can be determined by using Equation (45). The *ISF* determines the stress ratio based on the volumetric information of the fiber quantity and maximum and minimum volumes of the recommended fibers and their contributions to the stress factor.

$$ISF = \frac{\left(V_{Fiber}^{input} - V_{MIN}\right)}{\left(V_{MAX} - V_{MIN}\right)}\left(B_{MAX} - B_{MIN}\right) + B_{MIN} \tag{45}$$

where,

V_{MIN} is the minimum absolute volume fraction, %.

V_{MAX} is the maximum absolute volume fraction, %.

B_{MIN} is the minimum stress factor.

B_{MAX} the maximum stress factor.

All four of the above values can be found in Table 7 based on the specific fiber type.

Table 7: Experimentally determined limit values of stress factors for different types of fibers.

Fiber Type	**Specific gravity**	**Absolute volume fraction, %**		**Stress factor**	
		V_{MIN}	V_{MAX}	B_{MIN}	B_{MAX}
None	1.0	100.0	-	1.00	1.00
Synthetic Structural Fibers	0.92	0.194	0.477	1.24	1.39
Steel Fibers	7.80	0.304	0.502	1.10	1.46
Low Modulus Synthetic	0.92	0.097	0.194	1.00	1.05

The minimum and maximum possible absolute weight fractions are computed based on practical recommendations and are provided in Table 8.

Table 8: Recommended fiber content ranges.

Fiber type	**Recommended fiber content range (lb/yd^3)**	
	$W_{f,MIN}$	$W_{f,MAX}$
Synthetic Structural Fibers	3	7.4
Steel Fibers	40	66
Low Modulus Synthetic	1.5	3

The trial safety factor (SF^{Trial}) is the initial estimate for an equivalent stress ratio factor for a specific fiber type and is given by Equation (46). This consideration accounts for a safety factor in the stress factor:

$$SF^{Trial} = ISF - SF^{0}_{Fiber} \quad (46)$$

where,

SF_{Fiber}^{0} is an arbitrary safety factor of 0.05.

The maximum and minimum allowed factors are then checked using the following equations:

$$SF_{MIN} = \begin{cases} 1.0 & V_{Fiber}^{input} < V_{MIN} \\ SF^{Trial} & V_{Fiber}^{input} \geq V_{MIN} \end{cases} \quad (47)$$

$$SF_{MAX} = \min\left(SF^{Trial}, B_{MAX}\right) \quad (48)$$

The equivalent stress ratio factor (SF^{Final}) is determined by:

$$SF^{Final} = \max\left[1.0, \min\left(SF^{Trial}, B_{MAX}\right)\right] \quad (49)$$

The residual strength ratio characterizing the contribution of the fiber-reinforcement, R_{150}^{150}, is then given by:

$$R_{150}^{150} = SF^{Final} - 1 \quad (50)$$

4.6 Wheel Wander

For whitetopping projects with a 6-ft joint spacing, the critical stresses are located at the bottom of the PCC overlay in the wheelpath. Because wheels wander on the slabs, a fatigue adjustment factor is needed for slabs with a joint spacing greater than 4ft × 4ft to account for the effect of wheel wander ($F_{Wheelwander}$). Finite element modeling (FEM) indicates that the stress distributions at the bottom of the PCC overlay for different load locations match well. Therefore, the normalized stress distribution curve obtained from the case of 4-in PCC placed on top of 6-in HMA was selected to develop $F_{Wheelwander}$. Figure 9 presents the adjustment factors for wheel wander at reliability of 50% and the equation for $F_{Wheelwander}$ is described as

$$F_{Wheelwander} = 2.0405 \times SR^{-1.695} \quad (51)$$

where,

SR is thestress ratio as defined in Equation (42).

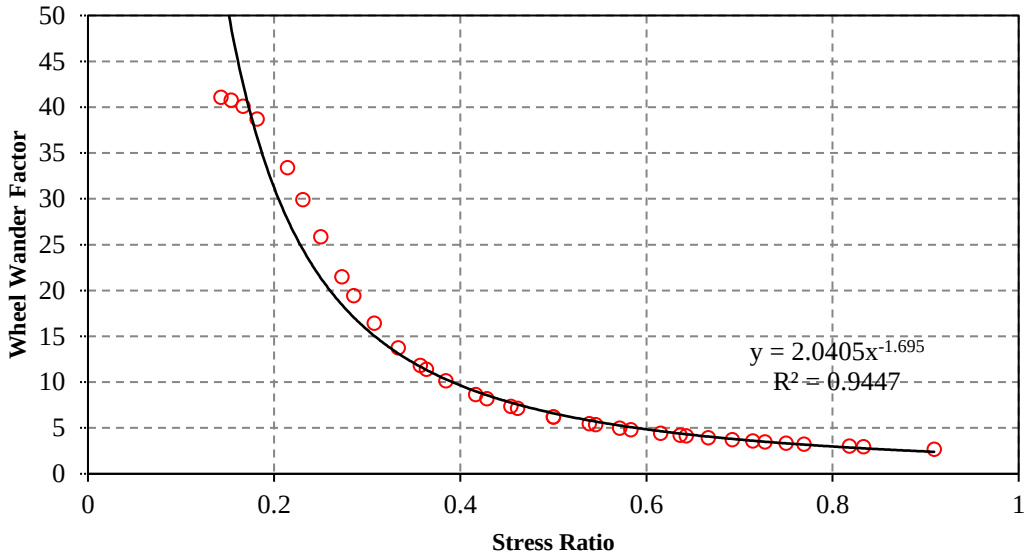

Figure 9: Fatigue adjustment factor for wheel wander in the design for slabs with joint spacing greater than 4ft × 4ft.

4.7 Stress Adjustment Factors

The stress adjustment factors are determined by calibrating the predicted performance in terms of fatigue damage to field distress measurements (percentage of slab cracking) using data from known whitetopping projects. Whitetopping projects listed in Table 9 are incorporated into the calibration database where 100% fatigue damage corresponds to 25% slabs cracked. Figures 10 and 11 show the adjustment factors generated by matching the predicted fatigue damage to the performance data of MnROAD Cells 93, 94, 95, 60 and 62.

The stress adjustment factors obtained for all projects in the database are then statistically correlated to pavement design features and are described by:

F_{stress} for slabs spanning the full lane width:

$$0.205h_{HMA} - 0.0296h_{PCC} + 0.65 \quad (52)$$

F_{stress} for a joint spacing greater than 4.5 ft and less than 7 ft:

$$\left(10^{1.44+0.45*h_{PCC}+0.02*h_{HMA}-5*\log(h_{PCC})-0.005*(h_{PCC})^2} + 0.4 + \frac{h_{PCC}}{9} + \frac{h_{HMA}}{40}\right) \cdot \left(\frac{650}{MOR}\right)^{0.5} \quad (53) \quad ($$

F_{stress} for a joint spacing less than or equal to 4.5 ft:

$$10^{\left[0.61073-0.1066\cdot\log\left(h_{pcc}\right)-0.705\cdot\log\left(h_{HMA}\right)+0.00861\cdot h_{HMA}^{2}\right]}\times\left(\frac{650}{MOR}\right)^{0.5} \quad (54)$$

Table 9: Whitetopping projects included in the calibration database for determining the stress adjustment factors.

State	Project	h_{PCC}, in	h_{HMA}, in	Slab size, ft × ft	F_{Stress}
Minnesota	Cell 95, MnROAD	3	10	6 × 6	2.20
	Cell 62, MnROAD	4	8	6 × 5	2.31
	Cell 60, MnROAD	5	7	6 × 5	2.20
	Cell 94, MnROAD	3	10	4 × 4	1.192
Missouri	Intersection of SR 291 and SR 78	4	4	4 × 4	2.00
	US-60 between US 71 and US 71 near Neosho	5	4.5	4 × 4	1.38
New York State	NY-408 and SH-622	4	9.5 (7)	4 × 4	0.77
Illinois	Highway 4- Piatt County	5	4	5.5 × 5.5	1.82
	Highway 2- Cumberland County	5.75	6.5	5.5 × 6	2.00
Colorado	US 85- Section1	4.7	4.5	5 × 5	1.55
	US 85- Section 2	5.8	5.9	5 × 5	1.80
	US 85- Section 3	6	5.4	5 × 5	1.85
	SH 119- Section 1	5.1	3.3	6 × 6	1.60
	SH 119- Section 3	6.3	3.4	6 × 6	1.84
	SH 119- Section 4	7.3	3.4	6 × 6	1.92

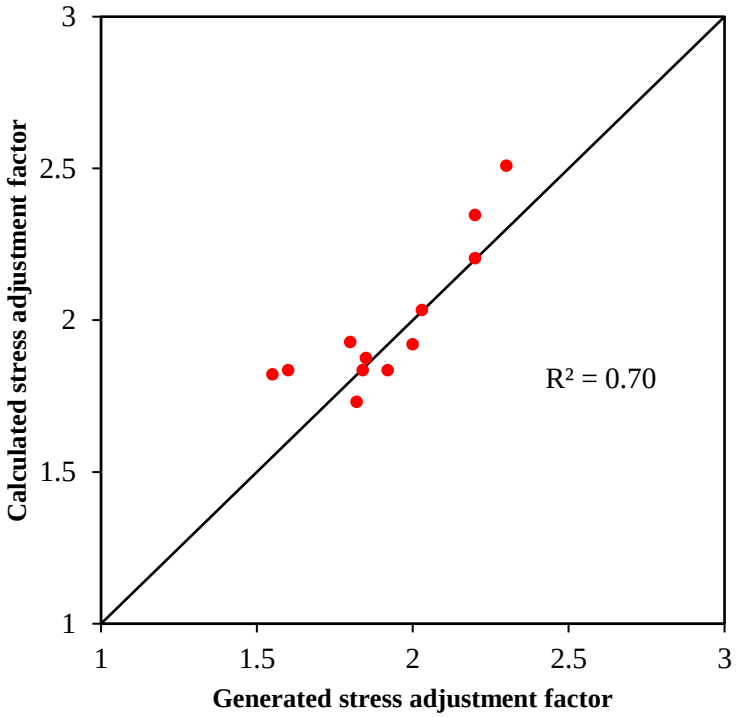

Figure 10: Stress adjustment factors for slabs with joint spacing greater than 4ft × 4ft.

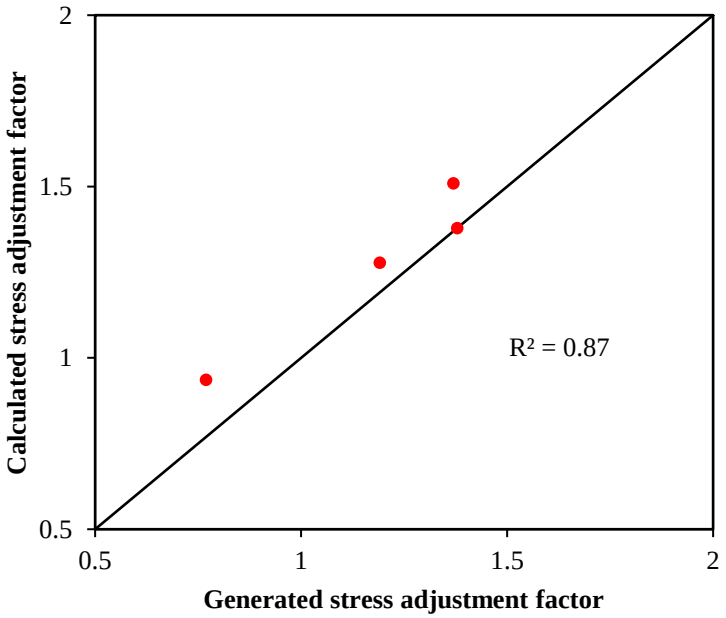

Figure 11: Stress adjustment factors for slabs with a joint spacing less than or equal to 4ft × 4ft.

Figures 12 to 15 present the performance data and the predicted fatigue of Cells 60, 62, 93, 94 and 95, respectively.

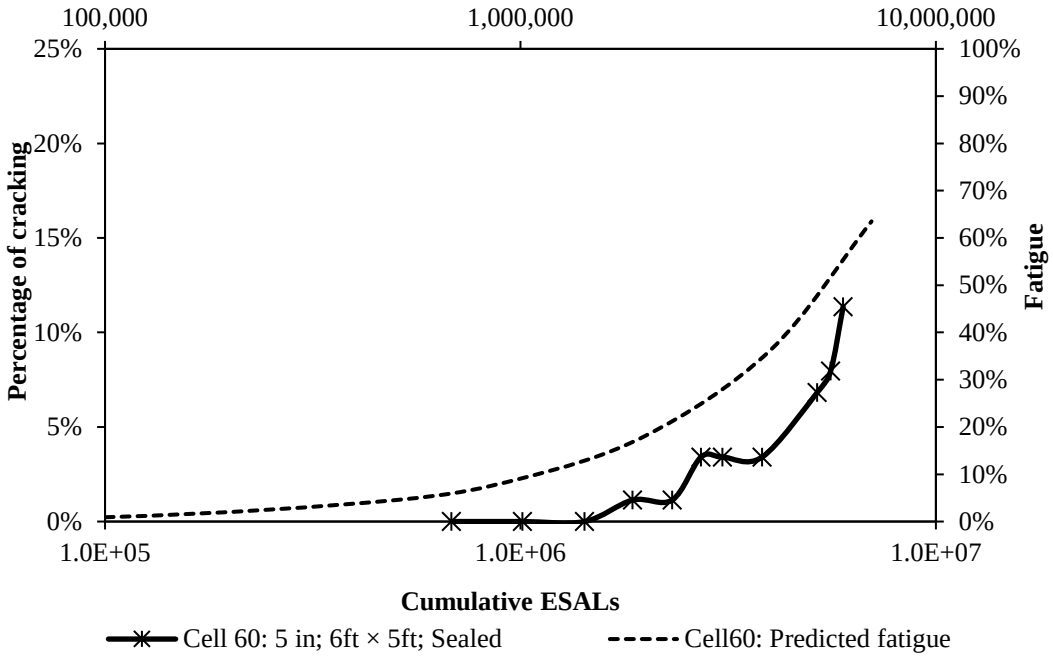

Figure 12: Performance data and predicted fatigue of Cell 60.

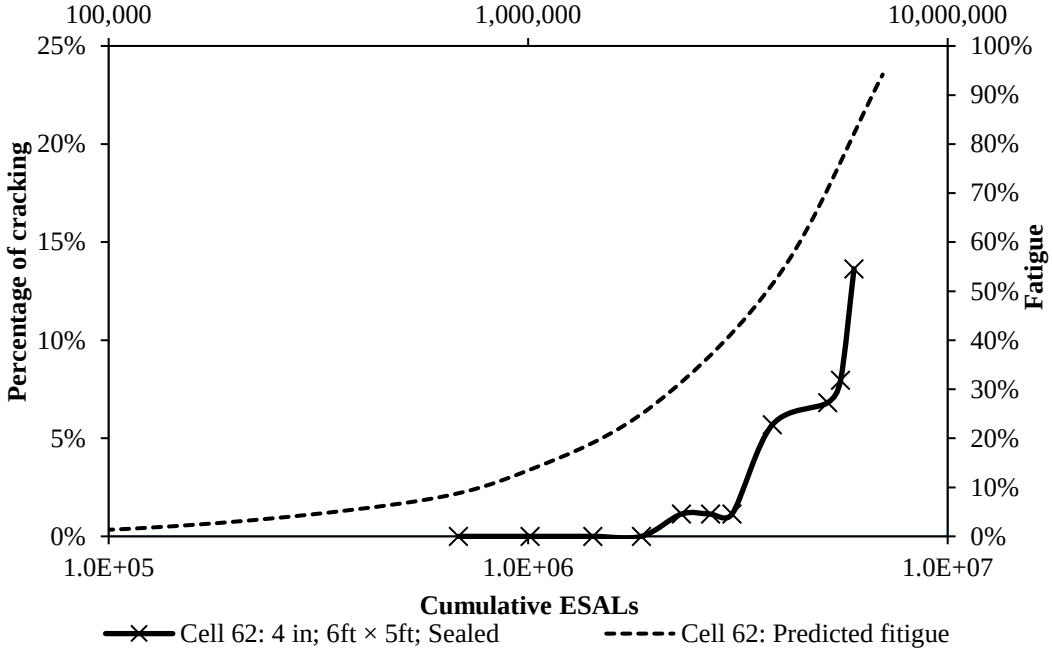

Figure 13: Performance data and predicted fatigue of Cell 62.

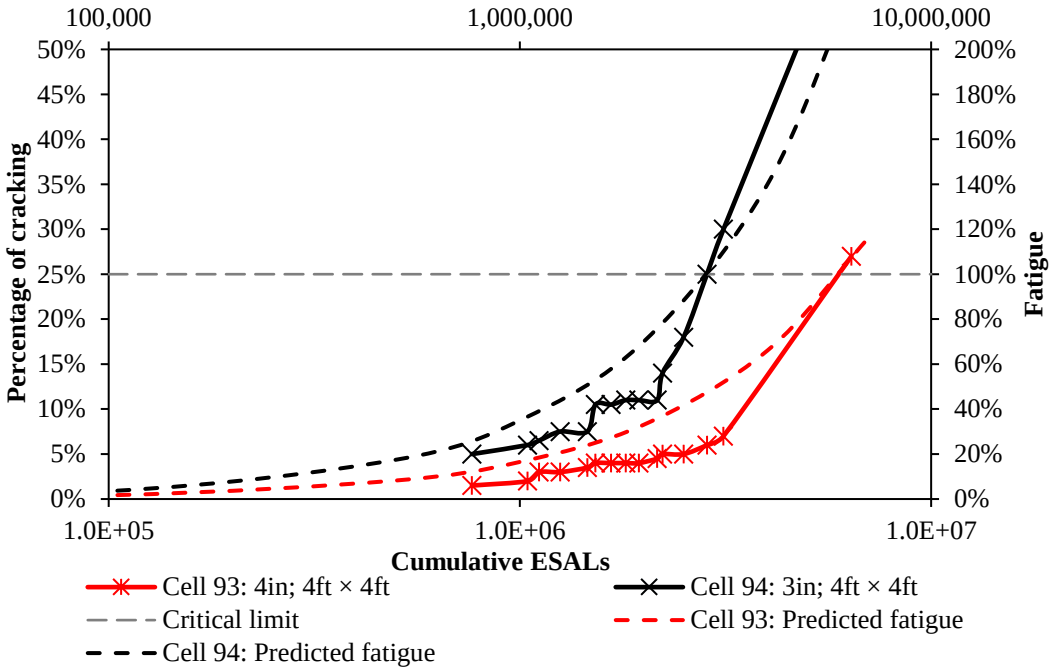

Figure 14: Performance data and predicted fatigue of Cells 93 and 94.

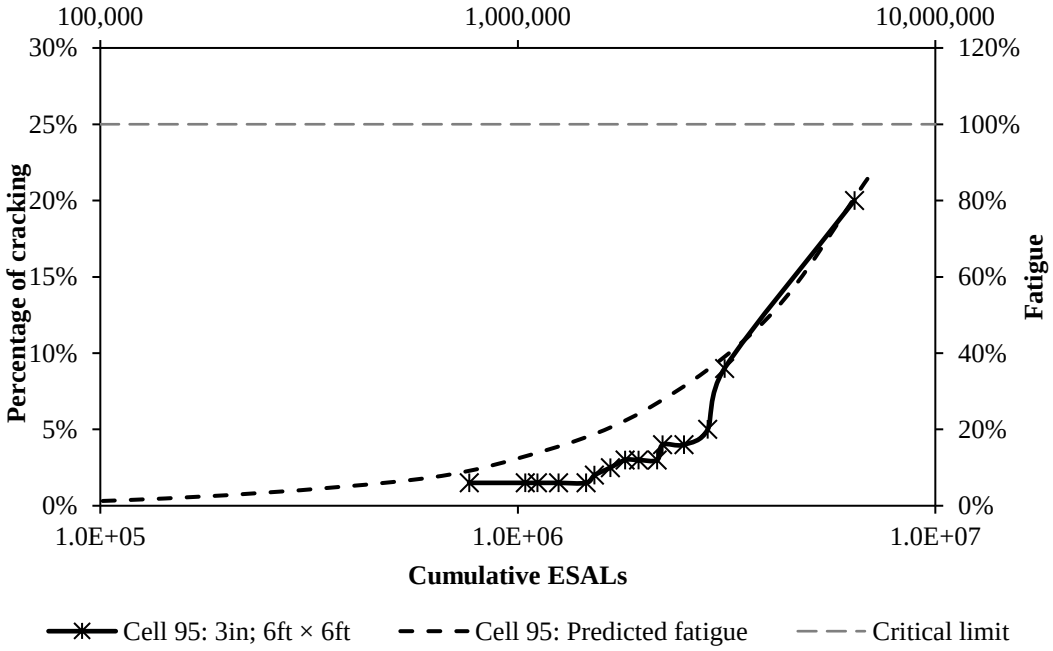

Figure 15: Performance data and predicted fatigue of Cell 95.

4.8 Reflective Cracking Potential

Reflection cracking occurs when the HMA layer undergoes thermal contraction in winter. This creates a stress concentration at the bottom of the concrete at the tip of any existing cracks in the

HMA. The magnitude of the tensile stress at the bottom of the concrete is then increased as a result of vehicle loads, thereby causing the crack in the underlying HMA to propagate up through the concrete overlay. Performance data from test sections shows that reflection cracking is a function of the relative stiffness of the HMA and PCC layers, as well as the accumulation of heavy traffic loads (Vandenbossche and Barman, 2010). The relative stiffness $D_{PCC/HMA}$ is calculated using Equation 55 below. BCOA sections with relative stiffness less than 1.0 will most likely experience reflective cracking.

$$D_{PCC/HMA} = \frac{E_{PCC} \times h_{PCC}^3}{E_{HMA} \times h_{HMA}^3}\left(\frac{1-\mu_{HMA}^2}{1-\mu_{PCC}^2}\right) \quad (55)$$

In the BCOA-ME model, the potential for reflective cracking is evaluated after the overlay thickness is evaluated. The estimated PCC thickness is then used to evaluate $D_{PCC/HMA}$, and the potential for cracking is reported as a binary result (yes or no) depending on whether $D_{PCC/HMA}$ is less than or greater than 1.0. This does not affect the predicted thickness of the overlay.

Some states have made the decision that the development of a few reflective cracks is acceptable, and they are not concerned with the effect of these cracks on the ability of the overlay to achieve its intended design life. If these reflective cracks are a concern, there have been methods identified to help prevent these cracks from reflecting into the overlay. Further information on these methods can be found in the Project Pathway Technical Note found in the BCOA-ME Practitioner's Information tool box on the BCOA-ME website.

4.9 Joint Sealing Effect

Performance data indicates that sealed whitetopping sections perform better than unsealed sections, as shown in Figure 16 (Burnham, 2013). Performance reviews of BCOA sections at MnROAD indicate that unsealed whitetopping sections would have an increase in PCC design thickness of approximately 0.5 in. This design procedure is developed using the sealed whitetopping design as the standard design.

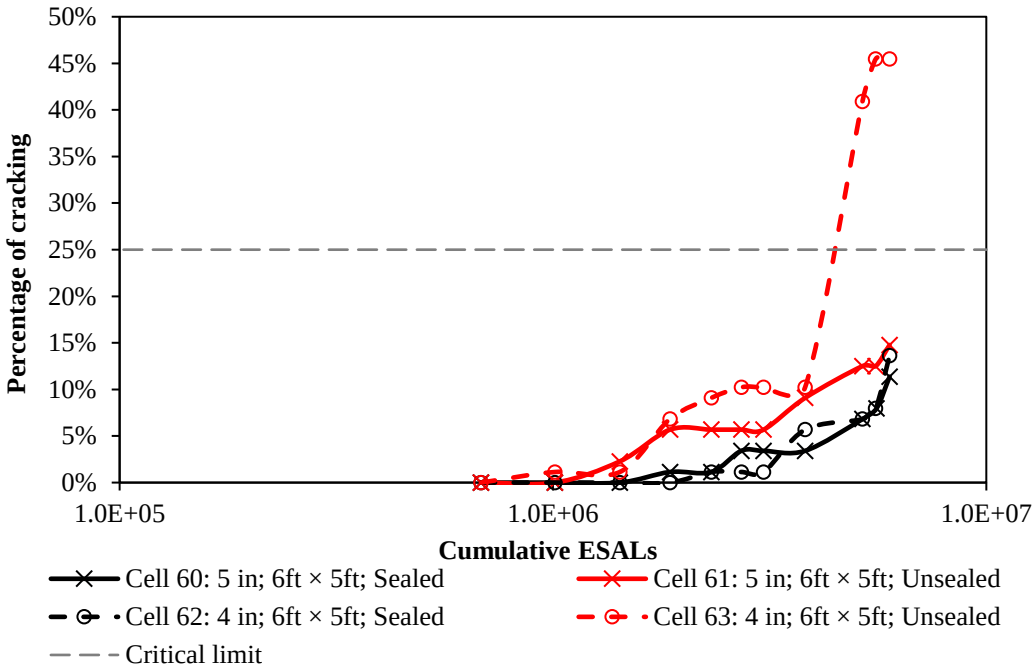

Figure 16: Performance data of sealed and unsealed sections in MnROAD.

5. Faulting Analysis

5.1 Differential Energy Concept

Faulting develops with the accumulation of traffic due to the pumping mechanism. Therefore, a model is necessary to predict the accumulation of damage undergone by the BCOA due to pumping. The present state of the practice for predicting faulting in jointed plain concrete pavements (JPCP) is based on the Differential Energy (DE) concept. DE relates the amount of elastic subgrade deformation under the loaded (L) and unloaded (UL) slabs to the development of faulting. The basic form of the DE concept can be seen in Equation (55).

$$DE = E_L - E_{UL} = \frac{k\delta_L^2}{2} - \frac{k\delta_{UL}^2}{2} \quad (56)$$

Where:

DE is the differential energy density of subgrade deformation, lb-in.

E_L is the density of elastic deformation of the loaded slab, lb-in.

E_{UL} is the density of elastic deformation of the unloaded slab, lb-in.

k is the modulus of subgrade reaction (combining the effects of all layers beneath the asphalt for BCOAs), psi/in.

δ_L is the corner deflection of the loaded slab caused by axle loading, in.

δ_{UL} is the corner deflection of the unloaded slab caused by axle loading, in.

In the present model, a 2 ft by 6 ft deflection basin was selected to characterize the pavement response in lieu of the more traditionally used corner deflection. Work by (DeSantis et al., 2019) showed the deflection basin better correlates with predicted deflection as compared to corner deflections. This basin size also accommodates the 6 ft by 6 ft slab size, which is commonly used in overlay design. It should be noted that faulting is not predicted for slabs shorter than 4.5 ft since insufficient performance data was available to characterize how faulting develops in BCOAs with these small slab sizes. A fractional factorial analysis was performed with models analyzed using the finite element method (FEM) to generate a database of whitetopping responses to a range of traffic and environmental loading conditions. The established critical response, along with corner deflections, were obtained for each analysis to train artificial neural networks (ANNs) (DeSantis and Vandenbossche, 2021 (In-press)).

5.1.1 Artificial Neural Networks (ANNs) Development

ANNs were established to be able to rapidly predict the critical response of a given whitetopping structure to be used to determine DE, as well as the joint shear capacity. These ANNs were established to predict the deflection basins for both the approach and leave side of the joint. In order to reduce the number of prediction models and to reduce the prediction variability between the different ANNs, the output of each ANN is the difference between the deflections on the approach (loaded) slab and the leave (unloaded) slab (basins and corners). This decreases the likelihood of an erroneous difference in prediction for the loaded and unloaded slabs (instead of two outputs, there is only one). Therefore, a total of 15 ANNs were trained, of which 10 ANNs were for partial lane-width panels, and 5 were for full-lane width panels; 6 ANNs for the deflection basins, 6 ANNs for corner deflections, and 3 ANNs for corner deflections based on temperature effects alone. These ANNs are separated into panel size based on the likelihood of the joint activation depth, axle type, and temperature loading. Due to symmetry of the temperature loading condition, only one ANN is necessary for both the loaded and unloaded sides of the joint (DeSantis et al., 2020).

The primary calculation for each month is to determine the DE, which can be found using Equations (56) and (59). The corner deflections due to traffic and environmental loading conditions are also used directly in the calculation of monthly incremental faulting and are evaluated from Equations (57) and (58) respectively.

$$\Sigma\delta_{B,A,m} = ANN_{\Sigma B,A,JD}(JTSpace, l_{eff}, q_i^*, k, \frac{AGG}{k * l_{eff}}, LTE_{shoulder}, s, \Phi) \quad (57)$$

$$\Sigma\delta_{C,A,m} = ANN_{\Sigma C,A,JD}(JTSpace, l_{eff}, q_i^*, k, \frac{AGG}{k * l_{eff}}, LTE_{shoulder}, s, \Phi) \quad (58)$$

$$\Sigma\delta_{C,T,m} = ANN_{\Sigma T,JD}(JTSpace, l_{eff}, 0, k, \frac{AGG}{k * l_{eff}}, LTE_{shoulder}, 0, \Phi) \quad (59)$$

$$DE_m = \sum_1^A \sum_1^j \sum_1^i (\frac{1}{2} k \left(\sum \delta_{B,A,m}\right) * WWpr_i * load_{A,j}) \quad (60)$$

Where:

$\Sigma\delta_{B,A,m}$ is the basin sum deflection for the difference between the loaded and unloaded slab for axle type A (A=1 for single; A=2 for tandem) for month *m*, in.

$\Sigma\delta_{C,A,m}$ is the corner deflection for the difference between the loaded and unloaded slab for axle type A (A=1 for single; A=2 for tandem) for month *m*, in.

$\Sigma\delta_{C,T,m}$ is the corner deflection for the loaded slab due to environmental loading only for month *m*, in.

$ANN_{\Sigma B,A,JD}$ is the ANN output for the difference between the squared sum of the 2-ft by 6-ft deflection basin for the loaded slab and the squared sum of the 2-ft by 6-ft deflection basin for the unloaded slab for axle type A (1 for single and 2 for tandem) and joint activation depth JD (0 for PCC only and 1 for full-depth), in^4.

$ANN_{\Sigma C,A,JD}$ is the ANN output for the difference between the corner deflection on the loaded slab and the unloaded slab for axle type A (1 for single and 2 for tandem) and joint activation depth JD (0 for PCC only and 1 for full-depth) , in.

$ANN_{\Sigma T,JD}$ is the ANN ouput for the corner deflection for the condition when only temperature is present for joint activation depth JD (0 for PCC only and 1 for full-depth), in.

$JTSpace$ is the joint spacing of the overlay, in.

l_{eff} is the effective radius of relative stiffness of the overlay, in.

q_i^* is the adjusted load/pavement weight ratio as defined below.

k is the modulus of subgrade reaction, psi/in.

$\frac{AGG}{k*l_{eff}}$ is the nondimensional joint stiffness.

$LTE_{shoulder}$ is the L/S joint load transfer efficiency (LTE), %.

s is wheel wander offset from the lane/shoulder (L/S) joint, in.

Φ is Korenev's non-dimensional temperature gradient as defined below.

DE_m is the differential energy density deformation accumulated for month *m*, lb-in.

$WWpr_i$ is wheel wander distribution over the number of bins *i*, in.

$load_{A,j}$ is the number of axles of axle type *A* at each load level *j*, where *A* is either a single or tandem axle, lb.

$$q_i^* = \frac{P_i}{A\,\gamma_{eff} h_{eff}}$$

where,

P_i is the axle load, lb.

A is the axle type parameter (1 for single axle and 2 for tandem axle).

h_{eff} is the effective thickness of the pavement, in.

γ_{eff} is the effective unit weight of the pavement, pci.

$$\Phi = \frac{2\alpha_{PCC}(1+\mu_{PCC})l_{eff}^2}{h_{eff}^2}\frac{k}{\gamma_{eff}}\,\Delta T$$

where,

α_{PCC} is the CTE of the overlay, in/in/°F.

μ_{PCC} is the Poisson ratio of the overlay.

ΔT is the temperature difference in the overlay (the product of the overlay thickness and EELTG), °F.

5.1.2 Special consideration for joint spacing

Joint spacing plays a particularly important role in the development of faulting since it determines whether the whitetopping undergoes faulting only within the PCC overlay (called partial-depth faulting) or both the overlay and underlying asphalt (called full-depth faulting). These two cases of joint activation, illustrated in Figure 17, lead to significantly different magnitudes of faulting since pumping occurs in either the asphalt layer or the subgrade, respectively (DeSantis et al., 2020). Furthermore, joint spacing also determines the joint opening width, a fact that is not considered in the finite element model.

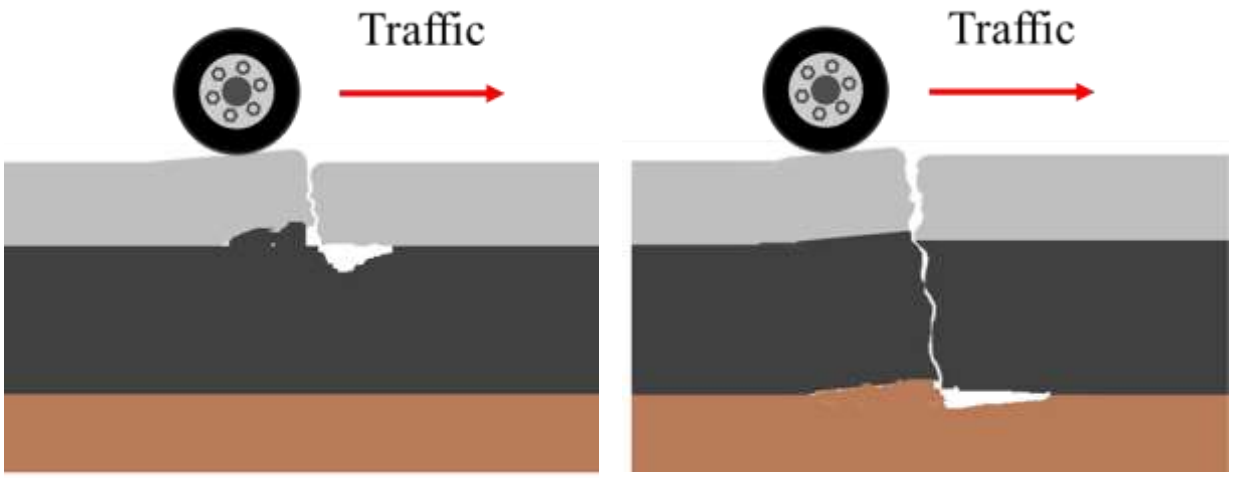

(a) Joint activation depth is through PCC only

(b) Joint activation depth is through PCC and asphalt

Figure 17: Faulting due to pumping of the different layers.

Therefore, for these reasons, the output of the ANNs are multiplied by a non-dimensionalized joint spacing, and the resulting deflection basin difference can be seen in Equation (60). This value is used to calibrate the faulting model, as discussed later.

$$\delta_{\Sigma B,A,JD} = \psi \frac{JTSpace}{h_{PCC}} [NN_{\Sigma B,A,JD}] \quad (61)$$

Where:

$\delta_{\Sigma B,A,JD}$ is the normalized deflection basin, in^4.

h_{PCC} is the thickness of the overlay, in.

ψ is a non-dimensional stability factor and is equal to 1.0 for medium slabs (joint spacing < 10 ft) and 0.01 for long slabs (joint spacing ≥ 10 ft). Short slabs (joint spacing ≤ 4.5 ft) are not considered in the faulting evaluation.

The ANNs were trained using outputs from a finite element analysis performed using ABAQUS and validated with whitetopping sections from the Minnesota Road Research Facility (MnROAD) (Cells 60, 96, and 97), as well as two sections from the University of California Pavement Research Center (UCPRC) heavy vehicle simulator (HVS) test sections (Sections B and F). Details can be found in (DeSantis and Vandenbossche, 2021).

5.1.3 ANN Predictors

The inputs related to traffic, EELTG, and HMA stiffness have been discussed in Sections 1-3, respectively. For traffic inputs, the same axle load spectra is used however, the predictors used in the development of the ANNs are axle loads instead of ESALs. The effect of these loads is evaluated monthly over the design life of the whitetopping. In addition, wheel wander is accounted for by using the national averages documented in the Pavement ME as Level 3 defaults for the average wheel location and standard deviation. Five wheel locations (mean location is 18 in from the outer edge of the lane/shoulder joint) with a standard deviation of 10 in are used within this framework.

Other inputs related to material properties are obtained directly as user inputs.

5.2 Faulting Model

The overall framework for relating DE to faulting is shown in Figure 18. Faulting – for both the full-depth and partial-depth joint activation –is evaluated incrementally each month by taking into account monthly DE, cumulative joint damage up to that month, and erosion potential. While DE has been discussed in detail in Section 5.0, the other two factors are discussed here before the faulting model itself is discussed.

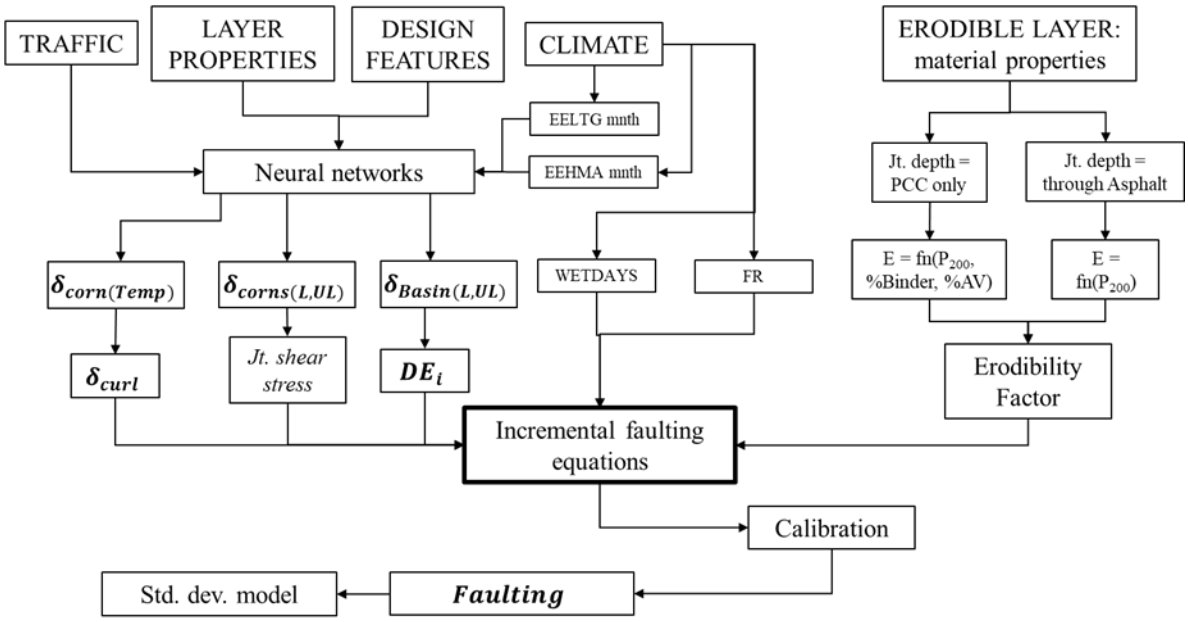

Figure 18: Flowchart for incremental prediction of faulting.

5.2.1 Joint damage and LTE

Joint LTE is a function of three mechanisms: aggregate interlock, dowel presence, and the underlying base layer (type, stiffness, and continuity). The LTE of the joint can be determined using Equation (61) and converted to *AGG* based on work by (Crovetti, 1994). This is a predictor used in the development of the ANNs.

$$LTE_{Joint} = 100\left[1 - \left(1 - \frac{LTE_{agg}}{100}\right)\left(1 - \frac{LTE_{dowel}}{100}\right)\left(1 - \frac{LTE_{base}}{100}\right)\right] \quad (62)$$

Where:

LTE_{agg} is the joint LTE if aggregate interlock is the only mechanism of load transfer, %.

LTE_{dowel} is the joint LTE if dowels are the only mechanism of load transfer, %.

LTE_{base} is the joint LTE if the base is the only mechanism of load transfer, %.

Aggregate interlock LTE is a function of joint width, which can be established using Equation (62). The concrete set temperature is estimated using the mean monthly temperature for the month of cast as well as the cement content. The concrete overlay shrinkage strain is established based on the tensile strength, which can be approximated using the compressive strength. The correlations adopted for these two properties are the same as is used in the AASHTO ’93 Design

Guide and are provided in in Equations (63) and (64). If a negative joint width is obtained, the joint opening is set to zero. It should be noted that the joint opening represents the width of the joint at mid-depth of the slab.

$$JW(m) = max\ (12000 * c * JTSpace * \left(CTE * \left(T_c - T(m)\right) + \varepsilon_{sh}\right), 0) \quad (63)$$

Where:

$JW(m)$ is the joint width for month *m*, mils.

c is the friction factor; 0.80 for stabilized layers (joint activation is PCC only), 0.65 for unstabilized layers (joint activation is through PCC and asphalt).

$JTSpace$ is the joint spacing in the overlay, ft.

CTE is the overlay PCC coefficient of thermal expansion, in/in/^{o}F.

T_c is the concrete set temperature, ^{o}F.

$T(m)$ is the mean mid-depth PCC overlay temperature for month *m*, ^{o}F.

ε_{sh} is the PCC overlay shrinkage strain, in/in.

$$f_c' = \left(\frac{E_{PCC}}{57000}\right)^2 \quad (64)$$

$$f_t' = 1.7 f_c'^{2/3} \quad (65)$$

where,

f_c' is the compressive strength of the concrete overlay, psi.

E_{PCC} is the elastic modulus of the concrete overlay, psi.

f_t' is the tensile strength of the concrete overlay, psi.

The non-dimensional aggregate joint stiffness can then be calculated for each month using Equations (65) and (66), adopted from (Zollinger et al., 1999). Note that ΔS_{tot} is equal to zero for the first month of the analysis and the individual monthly increments of loss in shear capacity can be calculated using Equation (67).

$$S = 0.5 * h_{PCC} * exp^{-0.032*JW} - \Delta S_{tot} \quad (66)$$

$$\log(J_{AGG}) = -3.19626 + 16.09737 * exp^{-exp^{-\left(\frac{S-e}{f}\right)}} \quad (67)$$

Where:

S is the dimensionless aggregate joint shear capacity.

h_{PCC} is the overlay thickness, in.

JW is the joint opening, mils.

$\Delta S_{tot} = \sum_{i=1}^{m} \Delta S_i$ is the cumulative loss of shear capacity at the beginning of the current month.

$J_{AGG} = (\frac{AGG}{k * l_{eff}})$ is the non-dimensional aggregate joint stiffness for the current month.

e is equal to 0.35.

f is equal to 0.38.

$$\Delta S_i = \begin{cases} 0 & if\ JW < 0.001 h_{PCC} \\ n_{i,A} * \dfrac{0.005 * 10^{-6}}{1.0 + \left(\frac{JW}{h_{PCC}}\right)^{-5.7}} \left(\dfrac{\tau_i}{\tau_{ref}}\right) & if\ 0.001 \le JW \le 3.8 h_{PCC} \\ n_{i,A} * \dfrac{0.068 * 10^{-6}}{1.0 + 6.0 * \left(\frac{JW}{h_{PCC}} - 3\right)^{-1.98}} \left(\dfrac{\tau_i}{\tau_{ref}}\right) & if\ JW > 3.8 h_{PCC} \end{cases} \quad (68)$$

Where:

ΔS_i is the loss of shear capacity from all ESALs for current month i.

$n_{i,A}$ is the number of axle A load applications for load level i.

h_{PCC} is the overlay slab thickness, in.

JW is the joint width opening, mils.

$\tau_i = J_{AGG} * (\Sigma \delta_{C,i,A})$ which is the shear stress on the transverse joint surface from the response model.

$\tau_{ref} = 111.1 * \exp(-\exp(0.9988 * \exp(-0.1089 * \log(J_{AGG}))))$ which is the reference shear stress derived from the PCA test results.

The doweled joint load transfer is only applicable for a doweled pavement, and was defined as shown in Equation (68) based on the existing model used in Pavement ME.

$$J_D = \frac{D}{\text{DowelSpace} \times k \times \ell} \tag{69}$$

Where:

J_D is the non-dimensional stiffnesses of doweled joints.

D is the shear stiffness of a single dowel (including dowel/PCC interaction), lb/in.

DowelSpace is the space between adjacent dowels in the wheel path, in.

The initial non-dimensional dowel joint stiffness is calculated using Equation (69) and the critical non-dimensional dowel joint stiffness is calculated with Equation (70) (ARA, 2004). The non-dimensional dowel stiffness is then calculated using Equation (71)**Error! Reference source not found.** and the cumulative dowel damage parameter is presented in Equation (72) (ARA, 2004).

$$J_0 = \frac{152.8 * A_d}{h_{pcc}} \tag{70}$$

$$J_d^* = \begin{cases} 118, & if \dfrac{A_d}{h_{pcc}} > 0.656 \\ 210.0845 \dfrac{A_d}{h_{pcc}} - 19.8, & if 0.009615 \leq \dfrac{A_d}{h_{pcc}} \leq 0.656 \\ 0.4, & if \dfrac{A_d}{h_{pcc}} < 0.009615 \end{cases} \tag{71}$$

$$J_d = J_d^* + (J_0 - J_d^*) exp\,(-DOWDAM) \tag{72}$$

$$DOWDAM = \frac{J_d * \left(\Sigma \delta_{C,A,m}\right) * DowelSpace * n_{i,A}}{d * f_c^{'}} \tag{73}$$

Where:

A_d is the area of dowel bar, in^2.

h_{pcc} is the overlay thickness, in.

J_0 is the initial non-dimensional dowel stiffness.

J_d^* is the critical non-dimensional dowel stiffness.

J_d is the non-dimensional dowel stiffness for current month.

$DOWDAM$ is the incremental dowel damage for the current month.

$DowelSpace$ is the dowel bar spacing, in.

$n_{i,A}$ = the number of axle A load applications for load level i.

d is the dowel bar diameter, in.

f_c' is the PCC compressive stress estimated from the modulus of rupture, psi.

Finally, the third mechanism that contributes to joint LTE is the underlying base layer. When a joint activates only through the PCC, the LTE_{base} is set equal to 30% (asphalt-treated or cement-treated). When a joint activates through both the PCC and asphalt, the LTE_{base} is set equal to 20% (aggregate base). In addition, the LTE of the joint increases if the pavement system is frozen. To account for this, when the mean monthly mid-depth PCC temperature is less than 32°F, LTE_{base} is set equal to 90%. The treatment of LTE_{base} follows the recommendations within the Pavement ME. The moisture level is indirectly accounted for through the WETDAYS parameter.

5.2.2 Erosion model

Two sets of incremental equations are used to determine faulting. The first set is for when the joint activates only through the PCC layer and the second set is for when the joint activates through both the PCC and asphalt layers. The difference between the two sets of equations is the treatment of the erodibility of the layer/material to undergo pumping. The erodibility factor of the layer being eroded away is also dependent on the depth of joint activation. If the joint is likely to only activate through the PCC layer, previously an erodibility value of one is assigned based on the erosion assessment established in the Pavement ME. However, a new approach was developed to account for the susceptibility to erosion based on the material properties of the asphalt layer, as shown in Equation (73).

$$E = E(\%\ eff.\ binder\ content, \%\ air\ voids, P_{200}) \quad (74)$$

Where:

% eff. binder content is the percent of effective binder content in the asphalt mixture. %.

% air voids is the percent of air voids in the asphalt mixture, %.

P_{200} is the percent of fines passing the number 200 sieve in a sieve analysis, %.

The exact form of E is established through the calibration process.

If the joint activates through both the PCC and asphalt layer, the erodibility classification established in the Pavement ME is adopted. Using this classification scheme and considering the typical properties of the materials present below the asphalt layer, an erodibility factor of four is assigned.

5.2.3 Incremental faulting equations

When the joint activates only through the PCC, faulting can be predicted using Equations (74)-(77).

$$F_0 = (C_1 + C_2 * FR^{0.25}) * \delta_{curl} * [C_5 * E]^{C_6} * log(WETDAYS * A\_P_{200}) \quad (75)$$

$$F_i = F_{i-1} + C_7 * C_8 * DE_i * [C_5 * E]^{C_6} \quad (76)$$

$$\Delta Fault_i = (C_3 + C_4 * FR^{0.25}) * (F_{i-1} - Fault_{i-1})^2 * C_7 * C_8 * DE_i \quad (77)$$

$$Fault_i = Fault_{i-1} + \Delta Fault_i \quad (78)$$

Where:

F_0 is the initial maximum mean transverse joint faulting, in.

FR is the base freezing index defined as the percentage of the time that the top of the base is below freezing (<32^{o}F).

δ_{curl} is the maximum mean monthly PCC upward slab corner deflection due to temperature curling and moisture warping, in.

E is the erodibility factor of the asphalt layer as a function of the asphalt mixture properties.

WETDAYS is the average number of annual wet days (> 0.1 in of precipitation).

A_P_{200} is the percent of aggregate passing No. 200 sieve of the asphalt layer, %.

F_i is the maximum mean transverse joint faulting for month *i*, in.

F_{i-1} is the maximum mean transverse joint faulting for month *i*-1 (in)(If i =1, $F_{i-1} = F_0$), in.

DE_i is the differential energy density accumulated during month *I*, lb-in.

$\Delta Fault_i$ is the incremental monthly change in mean transverse joint faulting during month *i*, in.

$C_1 \ldots C_8$ are the calibration coefficients.

$Fault_{i-1}$ is the mean joint faulting at the beginning of month *i* (0 if *i* = 1), in.

$Fault_i$ is the mean joint faulting at the end of month *i*, in.

When the joint activates through both the PCC and asphalt layer, faulting can be predicted using Equations (78)-(81).

$$F_0 = (C_1 + C_2 * FR^{0.25}) * \delta_{curl} * \left[log\ (1 + C_5 * 5^{EROD}) * log(\frac{P_{200} * WETDAYS}{\rho_s})\right]^{C_6} \quad (79)$$

$$F_i = F_0 + C_7 \sum_{j=0}^{m} DE_j * log\ (1 + C_5 * 5^{EROD})^{C_6} \quad (80)$$

$$\Delta Fault_i = (C_3 + C_4 * FR^{0.25}) * (F_{i-1} - Fault_{i-1})^2 * C_7 * DE_i \quad (81)$$

$$Fault_i = Fault_{i-1} + \Delta Fault_i \quad (82)$$

Where:

F_0 is the initial maximum mean transverse joint faulting, in.

FR is the base freezing index defined at the percentage of the time that the top of the base is below freezing (<32°F).

δ_{curl} is the maximum mean monthly PCC upward slab corner deflection due to temperature curling and moisture warping, in.

EROD is the erodibility of the layer beneath the asphalt.

P_{200} is the percent of aggregate passing No. 200 sieve of the layer beneath the asphalt, %.

WETDAYS is the average number of annual wet days (> 0.1 in of rainfall).

ρ_s is the overburden on the layer beneath the asphalt, lb.

F_i is the maximum mean transverse joint faulting for month *i*, in.

F_{i-1} is the maximum mean transverse joint faulting for month *i*-1 (if i =1, $F_{i-1} = F_0$), in.

DE_i is the differential energy density accumulated during month *i*, lb-in.

$\Delta Fault_i$ is the incremental monthly change in mean transverse joint faulting during month *i*, in.

$C_1 \ldots C_7$ are the calibration coefficients.

$Fault_{i-1}$ is the mean joint faulting at the beginning of month *i* (0 if i = 1) , in.

$Fault_i$ is the mean joint faulting at the end of month *i*, in.

When there is a section that is likely to have both depths of joint activation, the individual models need to be coupled together. Depth of joint activation depends on several factors, including the ration of the stiffness between the HMA and PCC layers, season, joint spacing, shrinkage, etc. After an extensive study of existing BCOA sections, it was concluded that joint spacing could be used as a convenient demarcation for joint activation. For medium-size slabs (joint spacing <10 ft), it was determined that approximately every sixth joint will activate full-depth (DeSantis et al, 2020). This may vary for different structures but is believed to be a suitable approximation. Therefore, the following equation is used to calculate average joint faulting for sections that have joints that activate to different depths.

$$Fault_m = \sum_{i=1}^{m} \left(\left(\frac{5}{6}\right) \Delta Fault_{PCC,i} + \left(\frac{1}{6}\right) \Delta Fault_{Full,i} \right) \quad (83)$$

Where:

$Fault_m$ is the mean joint faulting at the end of month *m*, in.

$\Delta Fault_{PCC,i}$ is the incremental monthly change in mean transverse joint faulting during month i when the joint is only through the PCC layer, in.

$\Delta Fault_{Full,i}$ is the incremental monthly change in mean transverse joint faulting during month i when the joint is through the PCC layer and the asphalt layer, in.

On the other hand, large-sized slabs (joint spacing ≥ 10 ft) were found to show full-depth joint activation only and the full-depth faulting model alone can be used for them.

5.3 Calibration

The calibration database used to calibrate the BCOA faulting model consists of 34 sections from five different states: Colorado, Illinois, Louisiana, Minnesota, and Missouri. The calibration sections are comprised of 18 sections at MnROAD, eight are sections from other areas across the state of Minnesota, five are sections in Colorado, and there is one section from Illinois, Louisiana, and Missouri. Initially, the calibration was limited to only sections within the state of Minnesota due to limited performance data. However, an ongoing National Cooperative Highway Research Program (NCHRP) study 1-61, "Evaluation of Bonded Concrete Overlays on Asphalt Pavements," aided in supplementing the calibration database. Although these sections only included one measurement of faulting, it was important to be able to include sections within the calibration dataset from outside of Minnesota.

Two separate calibrations needed to be conducted in order to account for the different trends in faulting due to the different depths of joint activation. Table 10**Error! Reference source not found.** presents a range of values for the entire calibration dataset for the more sensitive parameters, with details about individual sections used for calibrating both cases of joint activation shown in Tables 11 and 12. Of the sections, 29 are undoweled while the rest are doweled. The dowel diameter for the doweled sections were all 1 in. Considering the number of time series observations available, a total of 269 data points (PCC only joint activation = 154 and PCC and asphalt joint activation = 115) were available for calibration of the two models.

Table 10: Range of parameters for calibration sections.

Parameter	Minimum	Maximum	Average
Age, yrs.	3.0	27.0	10.4

Estimated ESALs	9.06E+04	1.91E+07	5.10E+06
Average joint spacing, ft	4	15	6
Overlay thickness, in	3	8	5
Overlay modulus, psi	3.60E+06	5.02E+06	4.40E+06
Overlay MOR, psi	507	902	685
Overlay cement content, lbs.	400	650	500
Existing asphalt thickness, in	3	16	8

Table 11: Calibration sections for joint activation through PCC only.

Section ID	**State**	**Overlay thickness, in**	**Asphalt thickness, in**	**Panel size, ft x ft**	**Dowel diameter, in**	**Estimated ESALs**
Cell 60_PCC	MN	5	7	5x6	None	8.45E+06
Cell 60_PL_PCC	MN	5	7	5x6	None	1.70E+06
Cell 96_PCC	MN	6	7	5x6	None	1.25E+07
Cell 96_PL_PCC	MN	6	7	5x6	None	3.50E+06
Cell 61_PCC	MN	5	7	5x6	None	8.45E+06
Cell 61_PL_PCC	MN	5	7	5x6	None	1.70E+06
Cell 62_PCC	MN	4	8	5x6	None	8.45E+06
Cell 62_PL_PCC	MN	4	8	5x6	None	1.70E+06
Cell 63_PCC	MN	4	8	5x6	None	8.45E+06
Cell 63_PL_PCC	MN	4	8	5x6	None	1.70E+06
06-83A	CO	8	16	6x6	None	5.91E+06
06-83B	CO	6	13	6x6	None	1.02E+07
06-121A	CO	6	13	6x6	None	3.13E+06
06-121B	CO	7	12	6x6	None	4.39E+06
17-27	IL	5	8	5.5x5.5	None	1.00E+07

22-167	LA	5	9	4x4	None	5.57E+06
29-60	MO	4.5	5	4x4	None	1.91E+07

Table 12: Calibration sections for joint activation through both PCC and HMA.

Section ID	**State**	**Overlay thickness, in**	**Asphalt thickness, in**	**Panel size, ft x ft**	**Dowel diameter, in**	**Estimated ESALs**
Cell 92_FULL	MN	6	7	10x12	1	1.16E+07
Cell 92_PL_FULL	MN	6	7	10x12	1	3.19E+06
CSAH 9	MN	7	6	15x12	1	4.35E+05
TH 56_2006-26	MN	6	8.5	15x13.5	1	9.06E+04
06-6	CO	6	9	10x12	1	4.69E+06
Cell 95_FULL	MN	3	10	5x6	None	4.76E+06
Cell 60_FULL	MN	5	7	5x6	None	8.45E+06
Cell 60_PL_FULL	MN	5	7	5x6	None	1.70E+06
Cell 61_FULL	MN	5	7	5x6	None	6.20E+06
Cell 61_PL_FULL	MN	5	7	5x6	None	1.14E+06
Cell 97_FULL	MN	6	7	10x12	None	1.16E+07
CSAH 7_43-607-14	MN	5	6	6x6,6x7	None	3.26E+05
CSAH 22_CP 12-14-22	MN	6	4	6x6	None	1.69E+05
CSAH 22_002-622-033	MN	6	4	6.25x6.25	None	1.28E+05
TH 30_0705-14	MN	6	7.5	12x12	None	3.39E+05
CSAH 22_02-622-31	MN	6	3	6x6, 6x7	None	2.26E+05
CSAH 2_43-602-(24-25)	MN	5	5	6x6, 6x7	None	2.19E+05

Calibration requires estimation of coefficients $C_1 - C_8$ introduced in Section 5.2.3 for both activation depths, as well as the erosion model in Equation (73), such that the overall error between the measured and predicted data was minimized.

For the erosion model, in addition to the sections listed in Table 11, additional data from several unbonded overlay (UBOL) sections were used to improve the fit. These sections are not listed in Table 11 but can be found in (Donnelly et al., 2021 (In Press)). The erodibility factor of these UBOL sections was scaled up to represent additional damage to the section, as would be the case for BCOA sections (UBOL is typically used for relatively less damaged sections as compared to

BCOA). The scaling factor was chosen empirically to obtain the best fit. The final fitted erosion model can be seen in Equations (83) and (84).

$$\alpha = \log\left(1 + a \times P_{200} + b \times \%AV + c \times (10 - \%Binder)\right) \quad (84)$$

$$E = \begin{Bmatrix} (-1.195\alpha^2 + 4.1115\alpha - 1.823) & Undoweled\ Pavements \\ (-1.016\alpha^2 + 3.495\alpha - 1.550) & Doweled\ Pavements \end{Bmatrix} \alpha > 0.56$$

$$E = \begin{Bmatrix} (0.108 * \alpha) & Undoweled\ Pavements \\ (0.091 * \alpha) & Doweled\ Pavements \end{Bmatrix} \alpha < 0.56 \quad (85)$$

Where:

α is the erodibility index.

a, b, c are the calibration coefficients (0.75, 0.06, and 0.17, respectively).

P_{200} is the percent aggregate passing No. 200 sieve for the asphalt, %.

$\%AV$ is the air voids percentage in the asphalt, %.

$\%Binder$ is the effective binder content of the asphalt, % (max. value =10%, if a value greater than 10% is specified, it should be lowered down to 10%. Values above 10% have a negligible effect on faulting.).

Predicted versus measured transverse joint faulting is presented for both models in Figure 19. Table 13 summarizes the calibration coefficients. In addition, the Pavement ME JPCP faulting national calibration coefficients are included for comparison purposes.

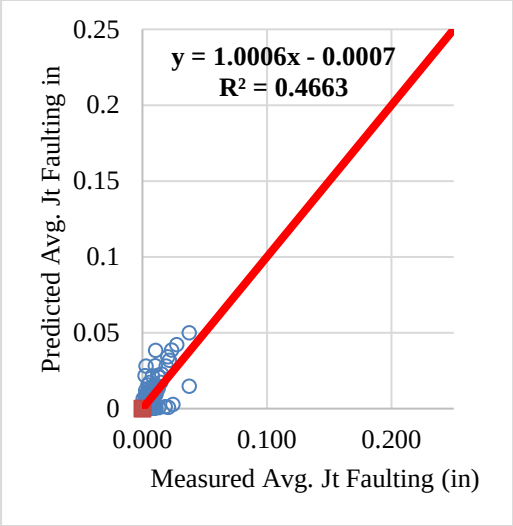

(a) Joint activates through PCC

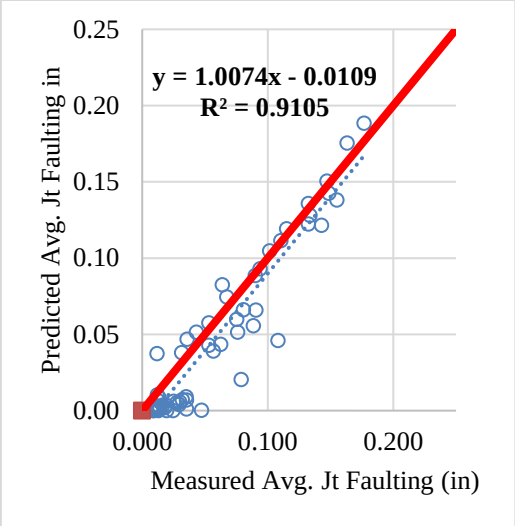

(b) Joint activates full-depth through PCC and Asphalt

Figure 19: Measured vs predicted faulting.

Table 13: Calibration coefficients.

Calibration coefficient	Joint activates through PCC	Joint activates full depth	Pavement ME initial	Pavement ME current
C_1	1.29	1.29	1.29	0.595
C_2	1.1	1.1	1.1	1.636
C_3	0.001725	1.0E-06	0.001725	0.00217
C_4	0.0008	1.0E-05	0.0008	0.00444
C_5	0.05	6.0E-04	250	250
C_6	2.2	4.275	0.4	0.47
C_7	3.245	1.27/5E-04	1.2	7.3
C_8	1/5E-06	-	400	400
Doweled: C_7	0.1	(48.0*dowel diameter)* C_7		

5.4 Reliability Model

Finally, the faulting predicted from the aforementioned model, which is at 50% reliability, needs to be scaled to a user-defined reliability R. The general model for this is as shown in Equation (85).

$$FAULT_R = FAULT - Stdev(FAULT) \times Z_R \quad (86)$$

Where,

$FAULT_R$ is the magnitude of faulting at the desired level of reliability R, in.

FAULT is the predicted faulting determined corresponding to 50 percent reliability, in.

Stdev(FAULT) is the standard deviation of the predicted faulting using the corresponding established reliability model, in.

Z_R is the standardized normal deviate corresponding to a reliability level R, presented in Table 14. Similar to the fatigue cracking model, 85% reliability is recommended.

Table 14: Reliability and corresponding standardized normal deviate.

Reliability, R (%)	**Std. normal deviate, Z_R**
50	0
75	-0.674
85	-1.037
90	-1.282
95	-1.645

The standard deviation model was developed similar to the methodology used in Pavement ME, and are shown in Equations (86) and (87) for joint activation through only the PCC layer and both the PCC and HMA layers respectively.

$$Stdev(FAULT\_PCC) = 0.1259 * (FAULT\_PCC^{0.5784}) \quad (87)$$

Where:

Stdev(FAULT_PCC) is the transverse joint faulting standard deviation when the joint only activates through the PCC, in.

FAULT_PCC is the predicted transverse joint faulting when the joint only activates through the PCC, in.

$$Stdev(FAULT\_FULL) = 0.0170 * (FAULT\_FULL^{0.1239}) \quad (88)$$

Where:

Stdev(FAULT_FULL) is the transverse joint faulting standard deviation when the joint activates through the PCC and asphalt layers, in.

FAULT_FULL is the predicted transverse joint faulting when the joint activates through the PCC and asphalt layers, in.

Figure 20 shows the goodness of fit of these models.

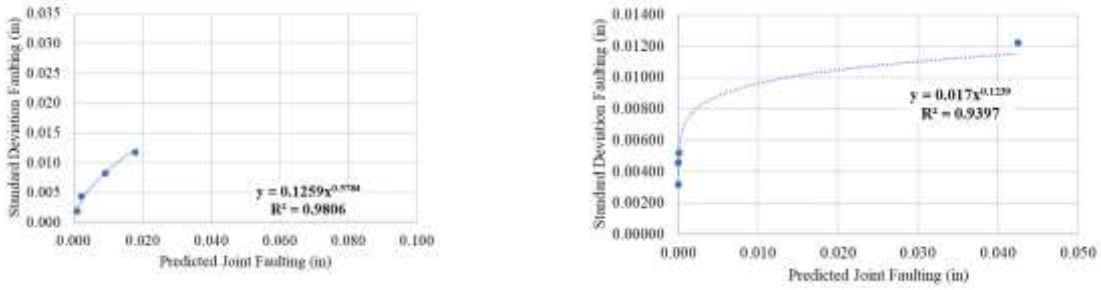

(a) (b)

Figure 20: Reliability models for joint activation through (a) PCC only and (b) both PCC and HMA.

5.5 Examples

Examples of measured and predicted faulting from some sections in MnROAD are shown in Figure 21. These include sections that experience joint activation through both the PCC and HMA layers (joint spacing $\geq$ 10 ft), and through the PCC layer only (joint spacing $<$ 10 ft). All of these sections, except Cell 95, were used to perform the calibration. Cell 95 is of particular interest since this section has fiber-reinforced concrete, which results in the observed faulting to be less than the predicted, since the presence of fibers is not currently accounted for in the faulting prediction model.

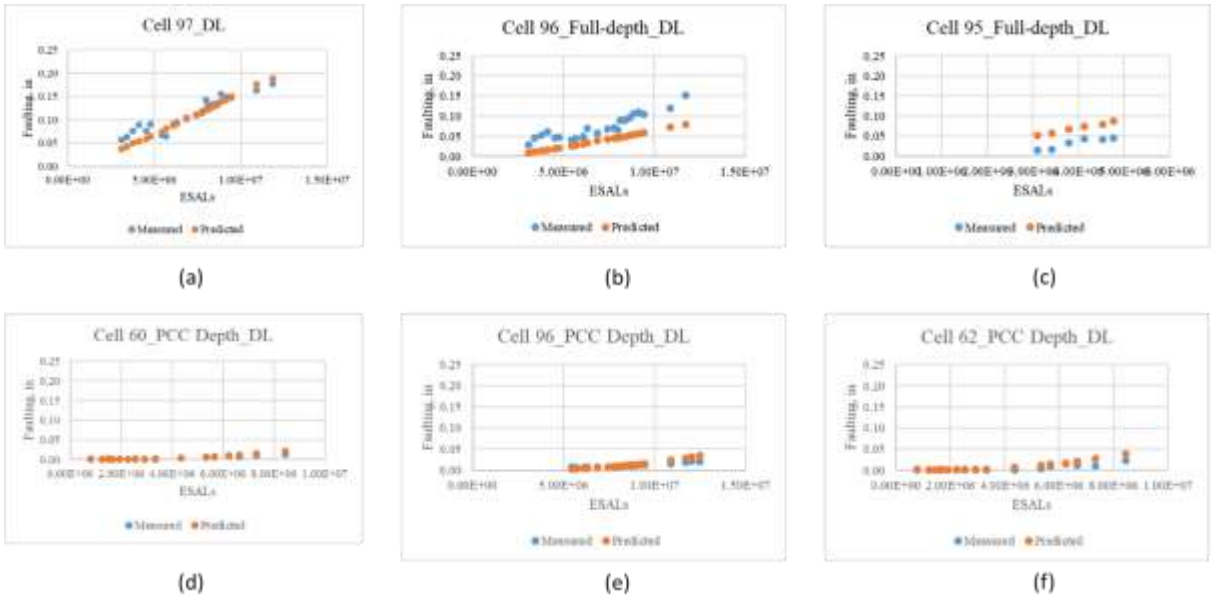

Figure 21: Predicted and measured faulting as a function of ESALs for MnROAD sections: (a)-(c) show faulting in sections with joint activation through both the PCC and HMA, while (d)-(f) through the PCC only.

Finally, some pictures from field sites where faulting was observed are shown in Figure 22.

Figure 22: Examples of whitetopping sections experiencing faulting (photos by Dr. John W DeSantis).

6. Conclusion

The BCOA-ME has been developed to provide a tool for predicting the overlay thickness for bonded concrete overlays over distressed HMA or composite pavements for a range of panel sizes. Previous procedures used for designing these structures were limited to the design of either UTW or TWT. This procedure allows the mode of failure to be dictated by the panel size and not the overlay thickness. In addition, the faulting model enables the designers to obtain an additional distress that has so far been absent from exiting tools despite it's importance to road quality and asset management. With the BCOA-ME, the designer has the ability to use one tool for the design of all bonded concrete overlays over HMA.

References

American Concrete Pavement Association (ACPA). *Design of Concrete Pavement for City Streets*. ACPA Publication IS184-P, American Concrete Pavement Association, Skokie, IL, 2002.

American Concrete Pavement Association (ACPA). *Whitetopping - State of the Practice*. ACPA Publication EB210P, American Concrete Pavement Association, Skokie, IL, 1998.

ARA, Inc. *Guide for Mechanistic-Empirical Design of New and Rehabilitated Pavement Structures*. National Cooperative Highway Research Program, Transportation Research Board, National Research Council, Washington, DC, 2004.

Mu, F. and J.M. Vandenbossche, "*Establishing Effective Linear Temperature Gradients for Bonded Concrete Overlays on Asphalt Pavements*," Transportation Research Record: Journal of the Transportation Research Board, *No. 2305*, TRB, National Research Council, 2012, pp. 24-31.

Burnham, T.R. *Forensic Investigation Report for Mn/ROAD Ultrathin Whitetopping Test Cells 93, 94 and 95*. Report MN/RC-2005-45, Minnesota Department of Transportation, St. Paul, MN, 2005.

Burnham, T.R. *Construction Report for Mn/ROAD Thin Whitetopping Test Cells 60-63*. Report MN/RC -2006-18, Minnesota Department of Transportation, St. Paul, MN, 2006.

Burnham, T.R. *The Effect of Joint Sealing on the Performance of Thin Whitetopping Sections at MnROAD*. Report MN/RC – 2006-18, Minnesota Department of Transportation, St. Paul, MN, 2013.

Crovetti, J.A. *Design and Evaluation of Jointed Concrete Pavement Systems Incorporating Open-Graded Permeable Bases*. Ph.D. Dissertation, University of Illinois at Urbana-Champaign, Urbana, IL, 1994.

DeSantis, J.W. *Modeling the Development of Joint Faulting for Bonded Concrete Overlays of Asphalt Pavements (BCOA)*. Ph.D. Dissertation, University of Pittsburgh, Pittsburgh, PA, 2020.

DeSantis, J. W., S. G. Sachs and J.M. Vandenbossche. "*Faulting Development in Concrete Pavements and Overlays*," International Journal of Pavement Engineering. 21(12), DOI:10.1080/10298436.2018.1548706, 2020, pp 1445-1460.

DeSantis, J.W., J.M. Vandenbossche, and S.G. Sachs. *Artificial Neural Networks for Predicting the Response of Unbonded Concrete Overlays in a Faulting Prediction Model.* Transportation Research Record, Vol. 2673, No. 10, 2019, pp. 762-769.

DeSantis, J.W., and J.M. Vandenbossche, "*Redevelopment of Artificial Neural Networks for Predicting the Response of Bonded Concrete Overlays of Asphalt in a Faulting Prediction Model*," *Transportation Research Record: Journal of the Transportation Research Board,* TRB, National Research Council, DOI:10.1177/03611981211001075, 2021.

Donnelly, C.A., J.W. DeSantis, J.M. Vandenbossche, and S.G. Sachs. *Mechanistic-Empirical Faulting Prediction Model for Unbonded Concrete Overlays of Concrete*. Transportation Research Record, 2021. (In Press)

Gucunski, N. *Development of a Design Guide for Ultra-Thin Whitetopping (UTW).* Report FHWA NJ 2001-018, New Jersey Department of Transportation, 1998.

Harrington, D. *Guide to Concrete Overlays: Sustainable Solutions for Resurfacing and Rehabilitating Existing Pavements*. National Concrete Pavement Technology Center, 2008, p. 69.

Larson, G. and B. Dempsey. *Enhanced Integrated Climatic Model Version 3.0 (EICM)*. University of Illinois, Urbana, IL, 2003.

Li, Z., and J.M. Vandenbossche. *Redefining the Failure Mode for Thin and Ultra-thin Whitetopping with 1.8-m by 1.8-m (6- x 6-ft) Joint Spacing*. Transportation Research Record, No.

2368, pp. 133-144, 2013.

Mindess, S., J.F. Young, and D. Darwin. *Concrete: Second Edition*. Pearson Education, Inc., 2003, pp. 312-217.

NOAA Satellite and Information Service. *Annual mean daily average temperature*. National Environmental Satellite, Data, and Information Service, http://cdo.ncdc.noaa.gov/climaps/temp0313, accessed Jan. 10, 2010.

National Renewable Energy Laboratory. *Annual Concentrating Solar Resource Map*. National Renewable Energy Laboratory, http://www.nrel.gov/gis/solar.html, accessed May 2010.

Pavement Systems, LLC. *LTTPBIND Version 3.1, a Superpave Binder selection program, developed by Pavement Systems LLC for Federal Highway Administration Asphalt Team – HTA-23*. Bethesda, MD, 2005.

Rasmussen, R.O. and D.K. Rozycki. *Thin and Ultra-Thin Whitetopping*. NCHRP Synthesis of Highway Practice 338, National Cooperative Highway Research Program, National Research Council, Washington, DC, 2004.

Riley, R.C., L. Titus-Glover, J. Mallela, S. Waalkes, and M. Darter. *Incorporation of Probabilistic Concepts into Fatigue Analysis of Ultrathin Whitetopping as Developed for the American Concrete Pavement Association*. Proceedings from the Best Practices in Ultra-Thin and Thin Whitetopping, Denver, Colorado, April 12-15, 2005, pp. 288-317.

Roesler, J., A. Bordelon, A. Ioannides, and M. Beyer. *Design and Concrete Material Requirements for Ultra-Thin Whitetopping*. Illinois Center for Transportation, Report No. FHWA-ICT-08-016, 2008, pp. E1-E26.

Sheehan, M.J., S.M. Tarr, and S. Tayabji. *Instrumentation and Field Testing of Thin Whitetopping Pavement in Colorado and Revision of the Existing Colorado Thin Whitetopping Procedure*.

Colorado Department of Transportation Research Branch. Report No. CDOT-DTD-R-2004-12, 2004.

Vandenbossche, J.M. *Performance Analysis of Ultrathin Whitetopping Intersections on US-169, Elk River, Minnesota*. Transportation Research Record, No. 1853, 2003, pp. 18-27.

Vandenbossche, J.M. and A.J. Fagerness. *Performance, Analysis, and Repair of Ultrathin and Thin Whitetopping at Minnesota Road Research Facility*. Transportation Research Record, No. 1809, 2002, pp. 191-198.

Vandenbossche, J.M. and Barman, M. *Bonded Whitetopping Overlay Design Considerations for Prevention of Reflection Cracking, Joint Sealing, and the Use of Dowel Bars*. Transportation Research Record, No. 2155, 2010, pp. 3-11

Wu, C.L., S.M. Tarr, T.M. Refai, M.A. Nagai, and M.J. Sheehan. *Development of Ultra-Thin Whitetopping Design Procedure.* Report RD 2124, Portland Cement Association, Skokie, IL, 1998.

Zollinger, D.G., N. Buch, D. Xin, and J. Soares. *Performance of CRC Pavements, Volume 6: CRC Pavement Design, Construction, and Performance.* Report FHWA-RD-97-151, Federal Highway Administration, Washington DC, 1999.